Can we use ice sheet reconstructions to constrain meltwater for deglacial simulations?

Ingo Bethke,[1,2] Camille Li,[1,2] and Kerim H. Nisancioglu[1,2]

Received 16 November 2011; revised 13 March 2012; accepted 14 March 2012; published 20 April 2012.

[1] Freshwater pulses from melting ice sheets are thought to be important for driving deglacial climate variability. This study investigates challenges in simulating and understanding deglacial climate evolution within this framework, with emphasis on uncertainties in the ocean overturning sensitivity to meltwater inputs. The response of an intermediate complexity model to a single Northern Hemisphere meltwater pulse is familiar: a weakening of the ocean overturning circulation in conjunction with an expansion of sea ice cover and a meridional temperature seesaw. Nonlinear processes are vital in shaping this response and are found to have a decisive influence when more complex scenarios with a history of pulses are involved. A meltwater history for the last deglaciation (21–9 ka) was computed from the ICE-5G ice sheet reconstruction, and the meltwater was routed into the ocean through idealized ice sheet drainages. Forced with this meltwater history, model configurations with altered freshwater sensitivity produce a range of outcomes for the deglaciation, from those in which there is a complete collapse of the overturning circulation to those in which the overturning circulation weakens slightly. The different outcomes are interpreted in terms of the changing hysteresis behavior of the overturning circulation (i.e., non-stationary freshwater sensitivity) as the background climate warms through the course of the deglaciation. The study illustrates that current uncertainties in model sensitivity are limiting in efforts to forward-model deglacial climate variability. Furthermore, ice sheet reconstructions are shown to provide poor constraints on meltwater forcing for simulating the deglaciation.

Citation: Bethke, I., C. Li, and K. H. Nisancioglu (2012), Can we use ice sheet reconstructions to constrain meltwater for deglacial simulations?, *Paleoceanography*, *27*, PA2205, doi:10.1029/2011PA002258.

1. Introduction

[2] The last deglaciation represents one of the largest climate shifts in recent history. Spanning a period of over 10 thousand years, it was a transition from the Last Glacial Maximum (LGM≈21 ka), when ∼120 m of sea level was tied up in massive continental ice sheets [*Fairbanks*, 1989; *Clark and Mix*, 2001; *Lambeck et al.*, 2002; *Peltier and Fairbanks*, 2006], to the warm and stable climate of the Holocene. Because the last deglaciation was a relatively recent event, its evolution is well documented in marine and terrestrial proxy records [*Sowers and Bender*, 1995; *Alley and Clark*, 1999]. Changes in insolation, continental ice sheets, and atmospheric greenhouse gas concentrations are known to be important in driving the transition from LGM to Holocene climate. More recently, there has been increasing interest in freshwater inputs to the ocean from the melting ice sheets, particularly with respect to the role they play in the rapid, high amplitude climate variability observed in the proxy records.

[3] Climate models have been used to investigate how the climate system evolves in response to these various forcings, and to assess their relative contributions in driving climate change throughout the deglaciation. As a first step, time slice simulations have been used extensively to study differences between the LGM and the present climate (and intervals in between) due to insolation, ice sheet and greenhouse gas forcing [*Broccoli and Manabe*, 1987; *Dong and Valdes*, 1998; *Ganopolski et al.*, 1998; *Bush and Philander*, 1999; *Lohmann and Lorenz*, 2000; *Hewitt et al.*, 2001; *Shin et al.*, 2003; *Singarayer and Valdes*, 2010], with much of this effort falling under the Paleoclimate Model Intercomparison Project [*Braconnot et al.*, 2004, 2007]. This time slice approach has demonstrated that, while reduced greenhouse gas concentrations contribute to cooler global mean temperatures at the LGM, polar amplification of LGM cooling and most of the large-scale atmospheric circulation changes can be attributed to the albedo (and topography) of the sea ice and land ice cover [*Rind*, 1987; *Justino et al.*, 2005; *Singarayer and Valdes*, 2010; *Pausata et al.*, 2009, 2011].

[4] Transient model studies allow an investigation of the time-evolving relationship between climate forcings and climate response, taking into account the nonlinear interactions that arise between different components of the climate system. From a practical standpoint, multimillennia simulations have

[1]Uni Research AS, Bergen, Norway.
[2]Bjerknes Centre for Climate Research, Bergen, Norway.

0883-8305/12/2011PA002258

for the most part been feasible only with computationally efficient set ups such as simplified or intermediate complexity model systems [*Lunt et al.*, 2006; *Timm and Timmermann*, 2007]. Such studies have provided assessments of the transient, accelerated and equilibrium climate response to transient insolation and CO_2 forcing as well as to changing continental ice sheets. For example, acceleration techniques are found to affect the large-scale, forced response in the high southern latitudes and the North Atlantic region, with maximum deviations of 2°C in the Southern Ocean compared to non-accelerated simulations [*Lunt et al.*, 2006]. More importantly for the purposes of this study, considering only the orbital, greenhouse gas and ice sheets forcings, the climate obtained in equilibrium time slice simulations is found to be a good match to the corresponding time period in a transient simulation [*Lunt et al.*, 2006]. *Lunt et al.* [2006] suggest that "over the last 30,000 years, the model's ocean-atmosphere system is close to equilibrium with its boundary conditions", at least when potentially slower responses from carbon cycle or vegetation changes are neglected. A similar conclusion was reached by *Timm and Timmermann* [2007], who find that the memory of the initial ocean state in transient deglacial simulations is lost after approximately 700 years. However, these results do not take into account the transfer of freshwater released to the ocean as the ice sheets melt.

[5] Accounting for freshwater from melting ice sheets is critical for simulating the deglaciation, but it is no trivial challenge. The title of this study asks whether this challenge can be met by using ice sheet reconstructions to constrain the meltwater forcing. Two sources of uncertainty hinder us. First is the uncertainty in the meltwater forcing history itself, an issue that is being addressed by ongoing and vigorous efforts in the data community. A second important source of uncertainty and the focus of this study is in the freshwater sensitivity of models.

[6] To comment briefly on the first source of uncertainty, reconstructing the deglacial meltwater forcing requires constraints on the timing, volume and location of the freshwater discharges associated with melting ice sheets. The importance of the timing and volume of the discharges is clear from studies showing that the model response to freshwater depends on the background climate [e.g., *Cheng et al.*, 2007; *Bitz et al.*, 2007; *Hu et al.*, 2008]. The importance of location (or partitioning) is demonstrated by studies that report different responses to idealized freshwater pulses in regions corresponding to different ice sheet drainages [e.g., *Mignot et al.*, 2007; *Otto-Bliesner and Brady*, 2010; *Roche et al.*, 2010]. One approach is to design hypothetical meltwater scenarios that produce the desired climate response—say, certain changes in Greenland temperature [*Alley*, 2000; *Rasmussen et al.*, 2006] or North Atlantic ventilation [*McManus et al.*, 2004]—such as was done recently by *Liu et al.* [2009] and *Menviel et al.* [2011] in transient model studies of the deglaciation. A different approach, and the one adopted in this study, is to construct a meltwater history based on reconstructions of the continental ice sheets throughout the deglaciation. The most commonly used ice sheet reconstructions are based on past sea level changes combined with the isostatic adjustment of Earth's crust to the unloading of continental ice masses [*Peltier*, 1994, 2004, 2009; *Argus and Peltier*, 2010]. Total ice sheet volume is constrained by global sea level curves at any given time; the volume of individual ice sheets is less certain, but measured crustal uplift rates provide partial constraints on when ice at specific locations melted. This meltwater may then be routed into the ocean through various drainages as indicated by geologic evidence, although the exact routings are the topic of active debate [e.g., *Teller*, 1990; *Marchitto and Wei*, 1995; *Clark et al.*, 2001; *Weaver et al.*, 2003; *Tarasov and Peltier*, 2005; *Peltier*, 2005; *Carlson*, 2009; *Murton et al.*, 2010]. This approach produces an objectively constructed deglacial meltwater history, but also one that is poorly constrained due to uncertainties in the ice sheet and drainage reconstructions and as well as the coarse temporal resolution (1 ky) of the ice sheet reconstruction.

[7] The second source of uncertainty is related to the freshwater sensitivity of climate models. While most climate models are able to produce realistic surface conditions for the present-day climate, they show less agreement in their simulation of the Atlantic Meridional Overturning Circulation (AMOC), a feature that is closely tied to the model response to freshwater. Only half of the models that contributed to the Coupled Model Intercomparison Project, Version 3 [*Meehl et al.*, 2007] exhibit a mean AMOC strength that lies within the observational estimates of 13–24.3 Sv (1 Sv $\equiv 10^6$ m^3 s^{-1}) [*Medhaug and Furevik*, 2011, Figure 6], and there are also discrepancies in the spatial structure of the AMOC [*Medhaug and Furevik*, 2011, Figure 5]. Models with a stronger overturning circulation tend to be more sensitive to freshwater [*Rahmstorf et al.*, 2005; *Stouffer et al.*, 2006], but there is a considerable spread in model behavior even after taking this trend into account. For example, in the model intercomparison study of *Stouffer et al.* [2006], the AMOC response to a 100 mSv freshwater forcing applied to the North Atlantic exhibits an absolute range of 1.3 to 9.7 Sv; when normalized relative to the mean AMOC strength of each model, the relative intermodel range is still over 100% of the ensemble mean response [*Stouffer et al.*, 2006, Figure 2]. There does not appear to be any simple relationship between model complexity or resolution and freshwater sensitivity [*Stouffer et al.*, 2006], and determining the causes for the intermodel differences (candidates include differences in mixing schemes and air-sea coupling) remains an active area of research [*Hofmann and Rahmstorf*, 2009]. For glacial conditions, there is little agreement among models as to the mean AMOC change relative to interglacial conditions [e.g., *Weber et al.*, 2007], although several studies (ours included) report higher model sensitivity to freshwater [*Ganopolski and Rahmstorf*, 2001; *Cheng et al.*, 2007; *Bitz et al.*, 2007; *Weber and Drijfhout*, 2007; *Hu et al.*, 2008]. Given that we are less equipped to produce reliable simulations of glacial climates than the present-day climate, especially for features such as deep water formation sites that are key for determining a model's freshwater sensitivity [*Smith and Gregory*, 2009], we should expect uncertainties in the AMOC response to freshwater perturbations in glacial conditions to be as large as, or larger than, uncertainties in present day conditions.

[8] The purpose of this study is to demonstrate that a wide range of deglaciation outcomes are possible due to uncertainties in how models respond to freshwater. We use just one model, but mimic the sum effect of mixing, boundary

layer and resolution errors by altering the sensitivity of the model to freshwater via constant, uniform salt fluxes (corresponding to negative freshwater fluxes of −100 mSv and −150 mSv) that are applied to the North Atlantic region. Additional experiments testing the effect of the changing background climate due to the other deglacial forcings (insolation, ice sheet extent and atmospheric greenhouse gas concentrations) are used to lend insight into the possible impact of errors in the timing of the pulses in the meltwater history. In particular, we are interested in the nonlinearity of the climate response to meltwater with multiple, transient sources, and how these nonlinear processes combined with the uncertainty in freshwater sensitivity of models can complicate attempts to simulate a complex, transient event such as the deglaciation. To understand past climate sensitivity to meltwater and to benchmark models against the past climate record, in turn, has potential relevance for constraining future thresholds with respect to Greenland and Antarctica ice sheet melt due to anthropogenic emissions.

[9] The paper is organized as follows. Section 2 describes the model system, transient forcings and experimental set-up. Section 3 presents the simulated transient background climate as a result of transient orbital, greenhouse gas and ice sheet extent forcings. Section 4 first assesses the model sensitivity to meltwater forcing, and then presents the transient response to the entire meltwater history for three alternative model configurations which represent high, intermediate and low sensitivity cases. The dependence on the transient background climate is investigated through a comparison with simulations with a fixed background climate state. Implications of our results for model-data comparison and future deglacial climate modeling are discussed in section 5, followed by conclusions in section 6.

2. Data and Methods

2.1. Model Description

[10] The MIT Integrated Global System Model Version 2 (IGSM2) comprises a 3-dimensional ocean general circulation model, a zonally integrated atmosphere-land model and a thermodynamic sea ice model [*Sokolov et al.*, 2005; *Dutkiewicz et al.*, 2005]. It is an earth system model of intermediate complexity and its high computational efficiency makes it particularly suitable for our study (for detailed discussions of advantages and disadvantages of this model type, see *Claussen et al.* [2002] and *Weber* [2010]). The model has been used in a wide range of applications, e.g., in coupled carbon cycle studies [*Sokolov et al.*, 2008] and for addressing future ocean circulation changes [*Scott et al.*, 2008]. The ocean component is the primitive equation model MITgcm [*Marshall et al.*, 1997], which in our configuration has a horizontal resolution of 4° and 15 vertical levels. The atmosphere-land component is a two-dimensional zonally averaged statistical-dynamical model that has a meridional resolution of 4° and 11 vertical levels. The sea ice component comprises a three layer thermodynamic sea ice model that is based on *Winton* [2000] and *Bitz and Lipscomb* [1999].

[11] The coupling between the ocean-sea ice and the zonally averaged atmosphere-land components is designed to obtain a realistic climate. Two-dimensional wind stress fields are constructed by adding the simulated zonal-mean wind stress anomalies (relative to model climatology) to an observational, monthly varying climatology [*Trenberth et al.*, 1990]. To obtain zonal variations in heat and evaporative fluxes, the zonal-mean surface fluxes are modified according to the flux derivatives with respect to surface temperature. Land runoff is collected into five zonal bands and then distributed to ocean grid cells according to contemporary river outflow data [*Perry et al.*, 1996]. The two-dimensional heat and freshwater flux fields are corrected with the help of a fixed flux adjustment [*Dutkiewicz et al.*, 2005]. All surface freshwater fluxes are applied as virtual salt fluxes.

2.2. Climate Forcings

[12] The model is forced with variations in insolation, atmospheric greenhouse gas concentrations, continental ice sheets and freshwater discharges into the ocean over the simulation period from 21–9 ka. Although insolation is the only true external forcing, we will use the term "forcing" for all of these model constraints.

[13] Figure 1 summarizes the transient forcings. Solar insolation (Figure 1a) is computed after *Berger* [1978] as a function of changing orbital parameters with the solar constant kept fixed at the modern value. Atmospheric greenhouse gas concentrations (Figure 1a) are prescribed according to CO_2 and CH_4 ice core data from Antarctica [*Monnin et al.*, 2001]. Ice sheets are prescribed according to the ICE-5G v1.2 reconstruction [*Peltier*, 2004], with extent changing but orography fixed at present-day values (i.e., parametrized atmospheric eddy fluxes are consistent with present-day orography [*Stone and Yao*, 1987, 1990]). For each latitude band, the ice sheet-covered land fraction is computed and then prescribed to the atmosphere-land model, which distinguishes between ocean, sea ice, land and land ice. The land ice fraction is updated every year with values obtained by linearly interpolating the 1 ky timeslices given in the ICE-5G data set. Changing surface type to ice-covered primarily affects the albedo, but also prevents summer temperatures from exceeding 0°C.

[14] Freshwater discharge from melting ice sheets is computed from ice volume changes between the 1 ky ICE-5G timeslices, assuming a linearly changing discharge rate from one timeslice to the next (Figures 1b and 1c). For simplicity, a density of $\rho_{ice} = 10^3$ kg m^{-3} is assumed during the conversion from ice to liquid freshwater, resulting in an overestimation of meltwater by ∼8%. A total volume of meltwater equivalent to ∼110 m of global sea level enters the ocean during the simulation period 21–9 ka. The discharge is routed to hosing regions (Figure 1e) known to be affected by freshwater via calving ice bergs or river outlets draining melting ice sheets, as described by *Roche et al.* [2010]. Routing from the Laurentide ice sheet is done purely by geography, by dividing the ice sheet into four catchment regions (Figure 1d): Atlantic (50N-85N, 100W-60W), Arctic (65N-85N, 170W-100W), Gulf of Mexico (30N-50N, 170W-50W) and Pacific (50N-65N, 170W-100W). While objective, the scheme is ad-hoc and the resulting idealized discharge scenario is an approximation of the one presented by *Peltier* [2004, Figure 10b]. Nevertheless, with a transient background climate, multiple discharge regions and a complete deglacial history of freshwater pulses, our study introduces a higher level of complexity than seen in most previous studies.

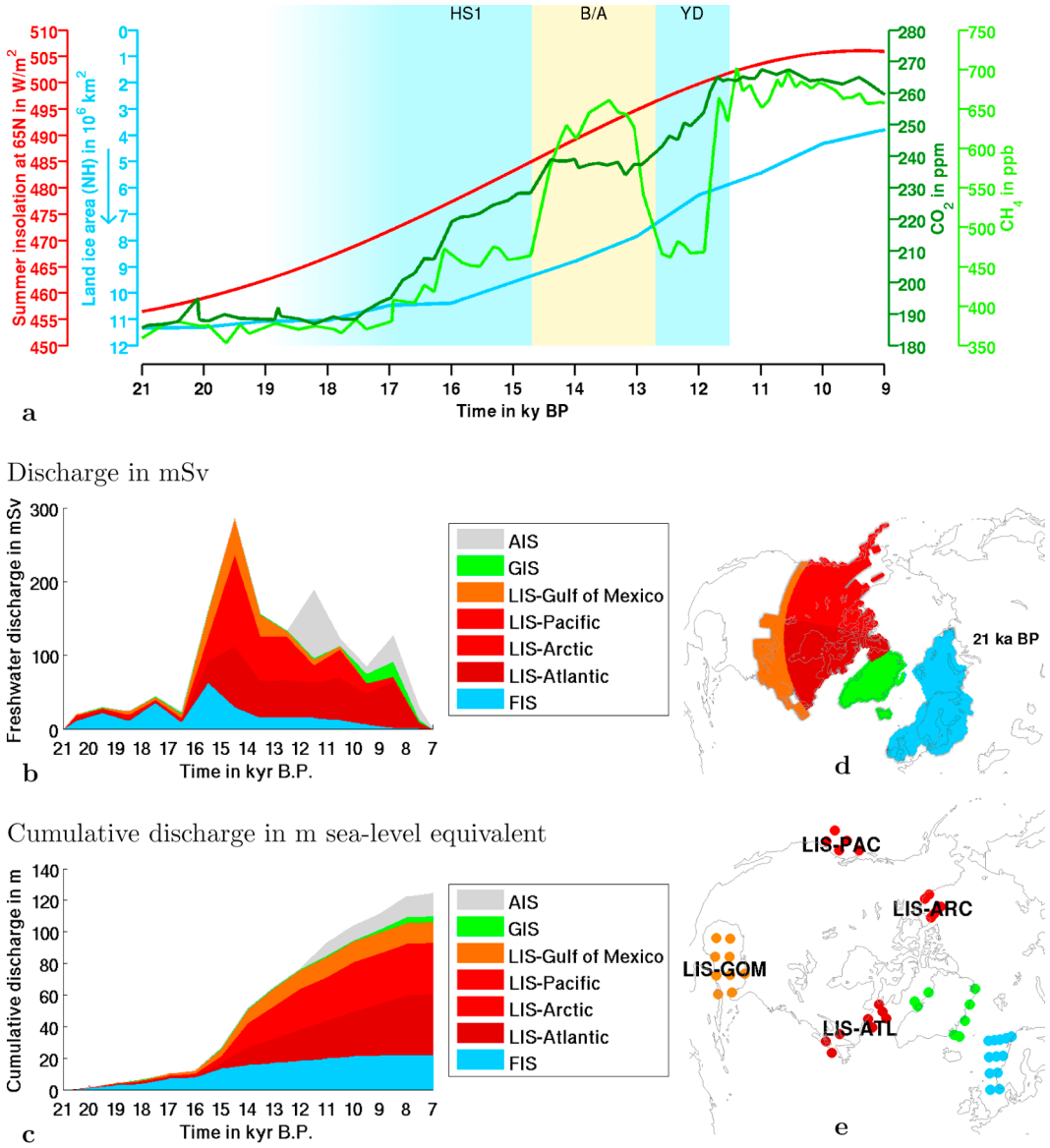

Figure 1. Climate forcings. (a) Atmospheric CO_2 concentration in green, land ice area in blue and June/July insolation at 65°N in red. The shading marks the Heinrich Stadial 1 (HS1) cold period (~18–15 ka), the Bølling-Allerød (BA) warm period (14.7–12.7 ka) and the Younger Dryas cold period (12.7–11.5 ka). (b) Implied meltwater discharge rates for the Fennoscandian Ice Sheet (FIS), Laurentide Ice Sheet (LIS), Greenland Ice Sheet (GIS) and Antarctic Ice Sheet (AIS). (c) Cumulative meltwater discharge. (d) LGM ice sheet extent and division into catchment areas. (e) Hosing regions that are similar to those of *Roche et al.* [2010].

[15] The main features of the discharge scenario as shown in Figures 1b–1e are as follows. Fennoscandian-sourced meltwater (including meltwater from the British and Barents Sea ice sheets) based on ICE-5G exhibits three 25–50 mSv (1 mSv = 10^3 m^3 s^{-1}) pulses occurring at approximately 20–19, 18–17 and 17–15 ka, followed by a 10–20 mSv tail persisting until 9 ka. The Fennoscandian contribution totals ~21 m sea level equivalent by the end of the deglaciation. There is relatively little Laurentide-sourced meltwater early in the deglaciation, but it increases rapidly after 16 ka and peaks around 15–14 ka at 250 mSv. This peak is known as meltwater pulse 1a (mwp1a), and while ICE-5G attributes it to the Laurentide, its origin is debated [*Clark et al.*, 1996; *Weaver et al.*, 2003; *Peltier*, 2005; *Stanford et al.*, 2006; *Carlson*, 2009]. In our deglacial scenario, approximately equal amounts of mwp1a are injected into the North Atlantic/Arctic and the Pacific Oceans, while considerably less enters the Gulf of Mexico (GOM). This partitioning overestimates the Pacific share from the Cordilleran ice sheet [cf. *Peltier*, 2005, Figure 5] and may underestimate the Arctic share [*Murton et al.*, 2010]. After mwp1a, discharge continues into the North Atlantic (approximately 50 mSv) until 9–8 ka, while discharge into the Pacific and GOM gradually declines, in agreement with *Marchitto and Wei* [1995]. Discharge from the Antarctic ice sheet exhibits a 50–100 mSv peak at 12–11 ka and a 10–25 mSv peak

Table 1. Experiment Overview[a]

Experiment Acronym	Climate Forcings							
	ghg	ice	orb	fw-fis	fw-lis	fw-gis	fw-ais	fw-20-50°N
Trend Experiments								
LGM	21k	21k	21k	–	–	–	–	–
GHG	**21→9k**	21k	21k	–	–	–	–	–
ICE	21k	**21→9k**	21k	–	–	–	–	–
ORB	21k	21k	**21→9k**	–	–	–	–	–
TRS	**21→9k**	**21→9k**	**21→9k**	–	–	–	–	–
Freshwater Experiments								
LGM+FIS	21k	21k	21k	**21→9k**	–	–	–	–
LGM+LIS	21k	21k	21k	–	**21→9k**	–	–	–
LGM+ALL	21k	21k	21k	**21→9k**	**21→9k**	**21→9k**	**21→9k**	–
TRS+FIS	**21→9k**	**21→9k**	**21→9k**	**21→9k**	–	–	–	–
TRS+LIS	**21→9k**	**21→9k**	**21→9k**	–	**21→9k**	–	–	–
TRS+ALL	**21→9k**	**21→9k**	**21→9k**	**21→9k**	**21→9k**	**21→9k**	**21→9k**	–
HYS^{21K}	21k	21k	21k	–	–	–	–	**−250⇌250 mSv**
HYS^{9K}	9k	9k	9k	–	–	–	–	**−250⇌250 mSv**

[a]Transient forcings are marked in bold.

at 9–8 ka. The Greenland ice sheet has only a small contribution at the end of the deglaciation after 10 ka with a magnitude of 10–20 mSv.

[16] Effects of vegetation changes [*Crowley and Baum*, 1997], volcanic influences on atmospheric aerosol load, orographic changes [*Justino et al.*, 2005; *Langen and Vinther*, 2009; *Eisenman et al.*, 2009; *Pausata et al.*, 2011], as well as sea level changes (ocean bathymetry is fixed at present day with an open Bering Strait) are not represented in this study.

2.3. Experimental Design

[17] The main results of this study are based on transient simulations from 21–9 ka using the deglacial forcings described above, either singly or in various combinations. An overview of all simulations is presented in Table 1.

2.3.1. Simulations of the Transient Background Climate

[18] Initial conditions are from the end of a 5,000 yearlong spin-up simulation that is initialized with climatological present-day fields and forced with fixed LGM (i.e., 21 ka) forcings. Three simulations GHG, ICE, and ORB are performed, where the simulation name indicates which forcing (greenhouse gas concentrations, ice sheet extent or orbital forcing) is transient (21–9 ka); the remaining two forcings are kept constant at 21 ka levels. Finally, simulation TRS includes fully transient greenhouse gas, ice sheet extent and orbital forcings.

2.3.2. Meltwater Simulations With Default Sensitivity

[19] The simulations that include meltwater discharge, either in a transient (TRS+ simulations) or fixed (LGM+ simulations) background state, are the main focus of this study, and are used to address the questions raised in section 1. The meltwater scenarios include ones in which there are discharges from the Fennoscandian ice sheet (FIS), the Laurentide ice sheet (LIS) and all ice sheets together (ALL).

2.3.3. Meltwater Simulations With Altered Sensitivity

[20] Two sets of simulations are performed where the overturning sensitivity is artificially reduced by adding a constant negative freshwater flux of either −100 mSv or −150 mSv to the latitude band 20–50°N across the North Atlantic. These simulations are labeled TRS^{100}+/LGM^{100}+ and TRS^{150}+/LGM^{150}+, with "TRS" or "LGM" indicating a transient or fixed LGM background climate, and the superscript indicating the amount of constant, negative freshwater flux. The freshwater flux applied to the North Atlantic is not compensated elsewhere. Global freshwater compensation has been found to affect the spatial signature of the climate response to NH freshwater forcing [*Stocker et al.*, 2007]. For the IGSM2, a compensated test simulation produces a qualitatively similar outcome compared to its uncompensated counterpart.

2.3.4. AMOC Hysteresis Simulations

[21] Finally, two standard AMOC hysteresis simulations HYS^{21K} and HYS^{9K} are performed with ice sheet extent, orbital parameters and greenhouse gas concentrations fixed at 21 ka and 9 ka levels, respectively. Following *Rahmstorf et al.* [2005], a freshwater flux is applied to the latitude band 20–50°N across the North Atlantic and is not compensated elsewhere. The magnitude of the flux is adjusted from −250 to 250 mSv and then back to −250 mSv at a rate of 50 mSv per 1,000 model years.

3. Simulated Transient Background Climate

[22] The simulated climate response to the slow deglacial forcings (i.e., forcings that vary on a multimillennial timescale) has been discussed in other studies [*Lunt et al.*, 2006; *Timm and Timmermann*, 2007; *Roche et al.*, 2011]. In this section, we present this response partly to validate the model and, more importantly because the change in background climate affects the climate sensitivity to freshwater forcing, as will be shown later. An important finding is that the simulated climate response to the slow forcings alone (i.e., no freshwater) is for the most part linearly additive, and therefore qualitatively different from the response to meltwater, which is strongly nonlinear and bears little resemblance to the forcing history.

[23] Figure 2 shows the temporal evolution of the response in global mean surface air temperature (SAT) and sea surface temperature (SST) to transient orbital, land ice area and greenhouse gas forcings. The global mean curves are plotted with the deuterium-based temperature reconstruction from the Antarctic EPICA ice core [*Jouzel et al.*, 2007]. Of the

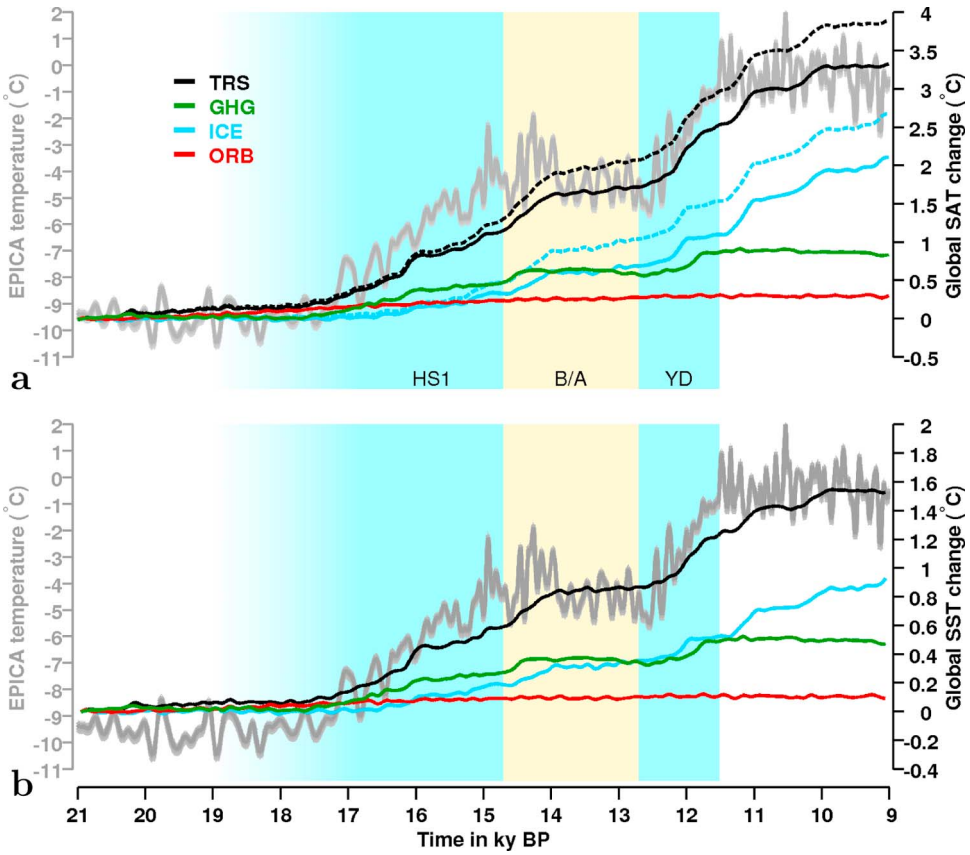

Figure 2. Global mean (a) SAT and (b) SST response to transient insolation forcing (red), ice sheet area forcing (blue), greenhouse gas forcing (green) and a combination of all three (black). Dotted lines denote an upper bound for the direct effect of ice sheet elevation changes estimated from orographic changes in ICE-5G using a fixed, adiabatic lapse rate of 9.8°C km^{-1}. The grey curve shows the deuterium-based temperature reconstruction from the Antarctic ice core EPICA [*Jouzel et al.*, 2007]. As a reference, global SAT changes are estimated to be approximately half of Antartic temperature changes [*Singarayer and Valdes*, 2010].

two locations where ice core records of the last deglaciation exist, Antarctica has been shown to be a better indicator of global changes than Greenland [*Masson-Delmotte et al.*, 2006; *Singarayer and Valdes*, 2010].

[24] The combination of transient orbital, greenhouse gas and ice sheet albedo forcing produces the general trend of the deglaciation as recorded in EPICA. Prior to 18 ka, the simulated global response is driven by solar insolation changes only. From 18 to 16 ka, greenhouse gas changes become important, followed by ice sheet area changes. From 14 ka onwards, the response to ice sheet area changes dominates, reaching 2°C in SAT and 0.9°C in SST by the end of the deglaciation. The latter is close to the 0.8°C warming obtained by *Broccoli and Manabe* [1987] with an atmospheric general circulation model coupled to a slab ocean model. Changes in surface albedo and ground properties due to the ice sheet retreat are responsible for most of the simulated temperature response. The response to orographic changes as a consequence of melting ice sheets is not included in the model (an upper bound estimate for the direct effect of ice sheet elevation changes is shown in Figure 2a, reaching a maximum of ~0.6°C at the end of the deglaciation). The total glacial-to-interglacial warming of ~4°C is within the 4–7°C range reported in the IPCC Fourth Assessment Report [*Jansen et al.*, 2007].

[25] The patterns of glacial-to-interglacial changes in SST, Atlantic Meridional Overturning Circulation (AMOC) and sea ice are shown in Figure 3. The surface warming is most pronounced in the Northern Hemisphere (NH) and parts of the Southern Ocean, and weaker in the tropics (Figure 3a). The NH warming is mostly due to ice sheet changes, while the greenhouse gas changes produce a more spatially uniform warming signature that is restricted to the upper ocean (not shown). The orbital changes have a relatively small effect in the global mean (Figure 2), but play a role in seasonal and hemispheric responses, in particular in the high latitude regions.

[26] The simulated global mean SAT and SST response to all three forcings in experiment TRS is approximately a linear combination of the individual responses in experiments GHG, ORB and ICE (Figure 2). There are a number reasons why the response to these slow forcings may be so linear, including the inability of the zonally averaged atmospheric model to capture atmospheric circulation changes, and the weak dynamical ocean response, a feature that has also been reported in other model studies [e.g., *Lunt et al.*, 2006]. Changes in the strength of the AMOC over the

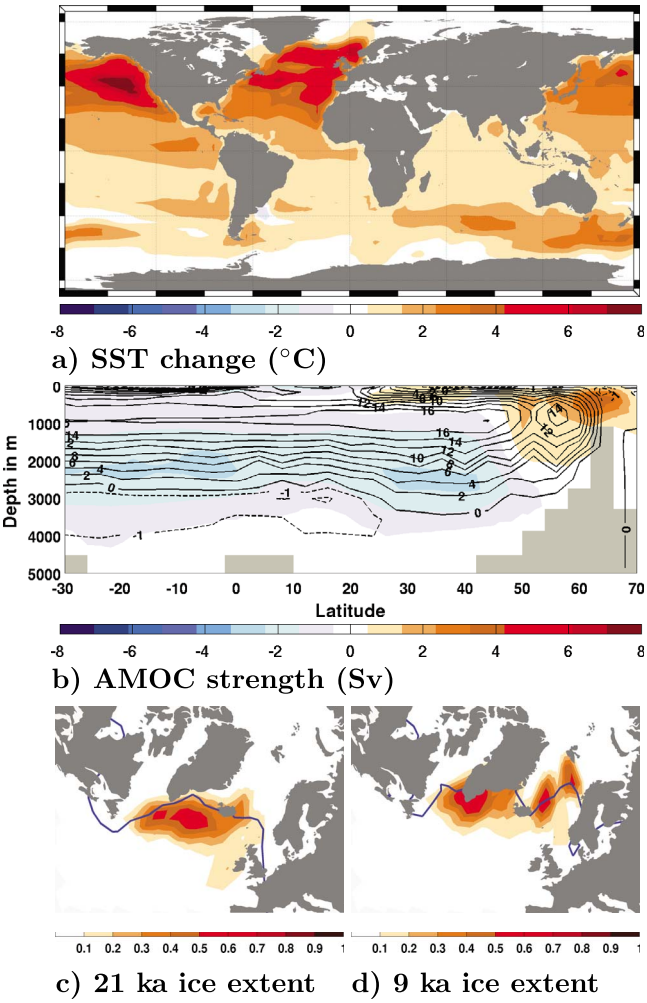

Figure 3. Spatial patterns of SST, AMOC, and NH sea ice changes in TRS. (a) The 9–21 ka difference in annual mean SST (°C). (b) AMOC stream function (Sv) at 21 ka (contours) and 9–21 ka difference (shading). (c) Sea ice extent in March (50% ice concentration contour) and fraction of time over the entire year that convection exceeds 500 m depth (shading) at 21 ka. (d) Same as in Figure 3c but for 9 ka.

deglaciation are less than 10% in the individual forcing experiments (not shown). TRS simulates a poleward migration of the overturning cell (Figure 3b), consistent with e.g., *Singarayer and Valdes* [2010], as a consequence of sea ice retreat and associated changes in deep wintertime mixing (Figures 3c and 3d), but also a slight shoaling of the AMOC (Figure 3b) that is at odds with marine proxy data [*Boyle and Keigwin*, 1987; *Duplessy et al.*, 1988; *Curry and Oppo*, 2005; *Lund et al.*, 2011]. Time slice simulations from other coupled models show a mix of AMOC changes between full glacial and pre-industrial conditions, including strengthening, weakening, deepening and shoaling [*Weber et al.*, 2007; *Otto-Bliesner et al.*, 2007]. The fact that the southern overturning cell is virtually absent in the simulations might bias our results, nor did we account for potentially important bathymetry changes due to the deglacial sea level rise [*Hu et al.*, 2007]. In light of the simplifications and weak dynamical ocean response described above, the simulations presented here must be considered idealized. Nevertheless, the model captures important features such as the retreat of the NH sea ice in combination with a northward extension of the overturning circulation and, as will be shown shortly, exhibits a transient meltwater sensitivity that is generally consistent with results from other model studies.

4. Effect of Uncertainties in Meltwater Constraints and Model Sensitivity on the Deglacial Evolution

[27] In this section, we investigate how model and forcing uncertainties associated with meltwater can impact the simulated evolution of a transient climate event such as the last deglaciation. The baseline simulation for these investigations is TRS+ALL, which covers the deglaciation from 21–9 ka and includes the full meltwater scenario involving all ice sheets. We will examine the relationship between the meltwater forcing and the climate response in this baseline case, as well as in additional experiments in which we alter the model sensitivity to meltwater, the background climate and the sources of meltwater discharge.

[28] First, we present the general features of the IGSM2 model response to freshwater, both the geographic response to a single pulse in the North Atlantic and the model sensitivity to North Atlantic freshwater input at the start (21 ka) and end (9 ka) of the deglaciation (section 4.1). In the following parts of the section, we investigate how errors in the model sensitivity to (section 4.2) and timing (relative to the transient background climate) of (section 4.3) the freshwater forcing can lead to very different outcomes in simulating the deglaciation. Together, these two cases illustrate the effects of translation (TRS+ versus TRS^{100}+ and TRS^{150}+ simulations) and deformation (TRS+ versus LGM+ simulations) of the AMOC hysteresis curve on transient climate simulations.

4.1. Response to Freshwater Forcing in the IGSM2

4.1.1. Single Freshwater Pulse

[29] As described in section 2, we construct the freshwater forcing as it is implied by the time evolution of the ICE-5G ice sheet reconstruction, with an idealized routing scheme based purely on geographical sectors (i.e., ice loss from a certain sector of the ice sheet is always routed through the same drainage to the same ocean region). Because most of the continental ice mass at LGM was in the NH, most of the freshwater discharge during the full deglaciation (110 m out of 125 m from 21 ka to present) entered the NH oceans (Figure 1). To first order, the simulated response to a given NH freshwater pulse is a weakening of the ocean overturning circulation leading to an interhemispheric temperature see-saw, a pattern that has been reported in previous modeling, observational and conceptual studies [*Crowley*, 1992; *Broecker*, 1998; *Stocker*, 1998; *Clark et al.*, 2002; *Knutti et al.*, 2004; *Stouffer et al.*, 2006].

[30] Figure 4 shows this characteristic response with a snapshot centered around the second freshwater pulse at 17.5 ka in the LGM+FIS simulation. The second pulse was chosen because it is well-isolated, has a simple, triangular shape (which facilitates the identification of characteristic response features) and has a larger amplitude than the first pulse (resulting in a more distinct response signal). During

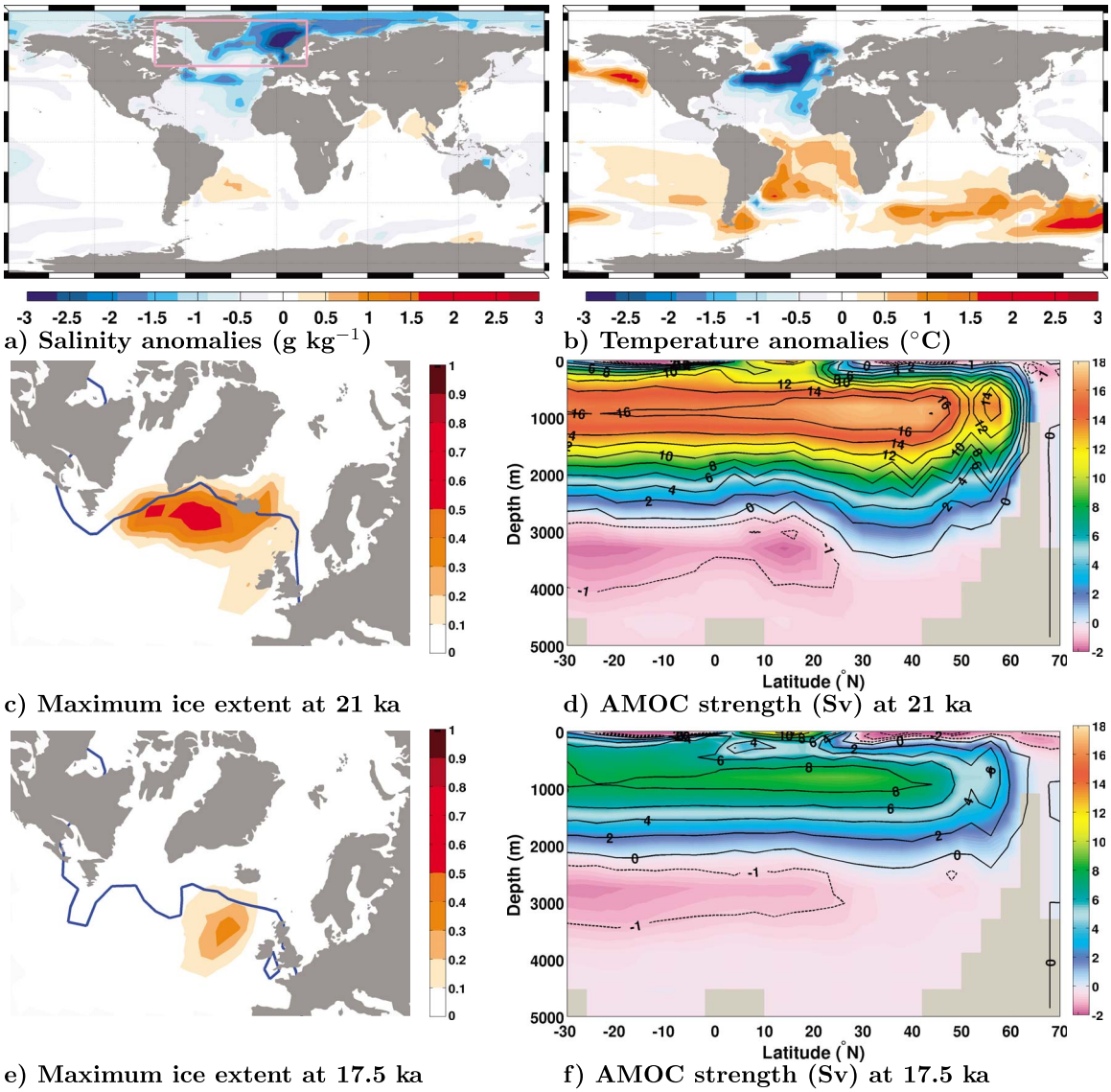

Figure 4. Climate response to a freshwater pulse from the Fennoscandian ice sheet in LGM+FIS. (a) The 17.5–21 ka difference in annual mean SSS (pink rectangle marks the region used for the computation of the time series in Figure 5). (b) The 17.5–21 ka difference in annual mean SST (°C). (c) Sea ice extent in March (50% ice concentration contour) and frequency of convection exceeding 500 m depth (shading) at 21 ka. (d) AMOC strength (Sv) at 21 ka. (e) Same as in Figure 4c but for 17.5 ka. (f) Same as in Figure 4d but for 17.5 ka.

the freshwater pulse, surface salinities are strongly reduced in the North Atlantic and Arctic. The SST signature is dominated by a north-south dipole anomaly in the Atlantic and a general warming of the Southern Ocean (Figure 4b). The surface cooling exceeds 3°C in the northern North Atlantic while the SH warming is less than 2°C. The NH winter sea ice edge expands south of the Greenland-Scotland Ridge (Figures 4c and 4e), where it inhibits surface heat exchange between the atmosphere and ocean. A basin-scale weakening of the AMOC is evident in the overturning stream function (Figures 4d and 4f). These gross features are similar to those in other freshwater hosing experiments [e.g., *Stouffer et al.*, 2006], but regional details are affected by the simplicity of our model system. For example, the low resolution of the ocean component limits its ability to resolve how anomalous freshwater is transported and affects dense water formation, and the zonally averaged atmosphere cannot represent atmospheric bridge processes found to link the North Atlantic and North Pacific in more complex general circulation models [*Cheng et al.*, 2007; *Krebs and Timmermann*, 2007].

[31] Figure 5 shows the temporal evolution of the freshwater pulse at 17.5 ka (Figure 5a) and the associated response (Figures 5b–5d). The climate response in surface salinity, AMOC strength (diagnosed as the maximum value of the AMOC stream function), and sea ice shows a markedly different behavior than the forcing, following neither the freshwater discharge rate nor the cumulative discharge, thus pointing to the importance of nonlinear feedback mechanisms in shaping the response. For example, surface salinity

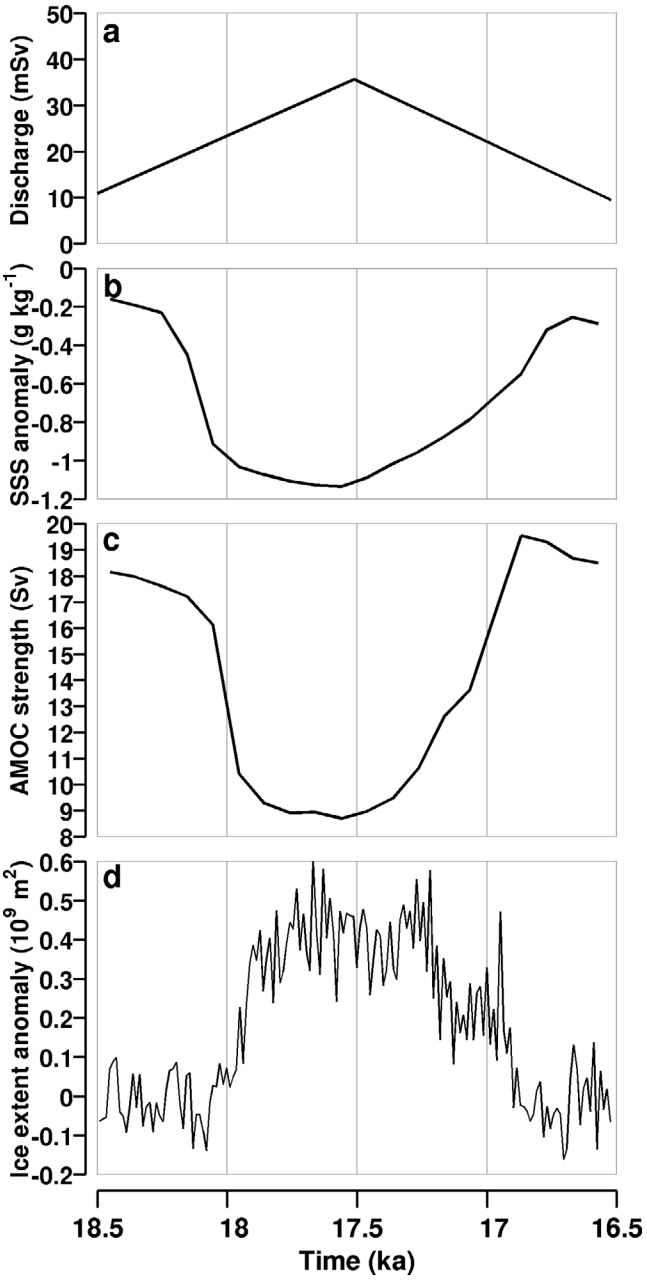

Figure 5. Temporal evolution of the climate response to a meltwater pulse from the Fennoscandian ice sheet in LGM +FIS. (a) Discharge rate of meltwater pulse (mSv), (b) box averaged (50N–80N, 80W–20E) surface salinity anomaly (g kg^{-1}), (c) AMOC (Sv), and (d) NH sea ice area (10^9 m^2).

averaged over 50N-80N, 80W-20E (Figure 5b) decreases abruptly after the initiation of the freshwater pulse, and remains in a freshened state up to 1 ka before it recovers. The presence of a fresher surface layer reduces winter mixing, impedes convection, and contributes to a weakening of the overturning circulation (Figure 5c) which in turn delays the export of the freshwater anomaly [*Weber and Drijfhout*, 2007]. Additionally, the enhanced stratification limits vertical redistribution of the freshwater anomaly. These positive feedbacks amplify the initial freshening and account for the similarity between the salinity and overturning time series (Figures 5b and 5c), which resemble each other more than they do the discharge curve (Figure 5a).

[32] Finally, changes in sea ice cover (Figure 5d) mirror the changes in surface salinity (Figure 5b) and overturning strength (Figure 5c). Surface salinity changes exert a direct influence on sea ice extent since open ocean sea ice cover requires the presence of a strong halocline to protect the ice from the relatively warm North Atlantic water masses below [*Bitz et al.*, 2005]. The expanded sea ice also provides a positive feedback on the surface freshening and weakened overturning by reducing wind stirring and surface heat loss, thereby enhancing surface stability, as indicated by the suppression of deep mixing in the western North Atlantic and Irminger Sea (Figures 4c and 4e).

4.1.2. AMOC Hysteresis

[33] The hysteresis diagrams (Figure 6) summarize key characteristics of the model overturning sensitivity to North Atlantic freshwater inputs at the beginning (HYS^{21ka}) and end (HYS^{9ka}) of the simulation period. These hysteresis curves are well within the range of those reported in existing model studies [*Rahmstorf et al.*, 2005, Figure 2], both in terms of the width and the position of the zero line which marks the unperturbed state. Doubling the rate of change of freshwater flux in the HYS^{9K} experiment produces curves with a similar shape, but exhibiting an earlier collapse and a slightly larger overshoot.

[34] The unperturbed state, where the stable (upper) branch of the hysteresis curve crosses the zero freshwater input line, does not change much during the course of the deglaciation; the AMOC strength at 9 ka is only ~1 Sv weaker than at 21 ka. However, the linear sensitivity to freshwater forcing near the unperturbed state (i.e., the slope in the stable regime) is slightly steeper at 21 ka than at 9 ka, such that the curves cross when the freshwater forcing is increased to ~100 mSv. The 21 ka overturning circulation collapses rather abruptly around this 100 mSv point, while

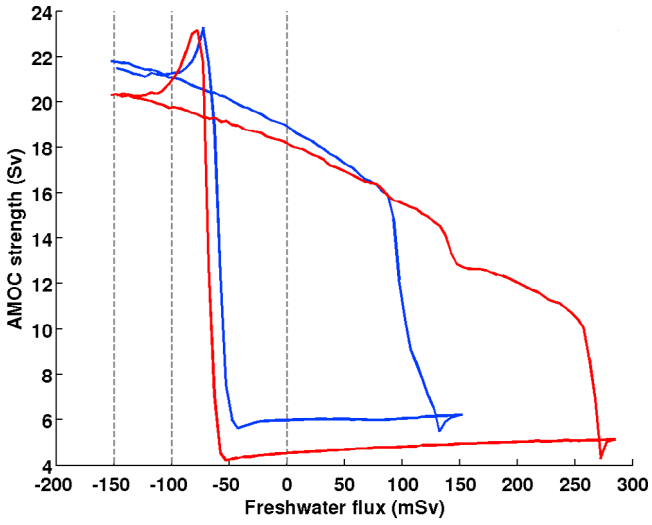

Figure 6. AMOC hysteresis. AMOC strength (Sv) for HYS^{21k} (blue) and HYS^{9k} (red) experiments as a function of freshwater flux to the Atlantic between 20–50°N. Dashed grey lines mark the zero lines for the experiments TRS^{150}, TRS^{100} and TRS.

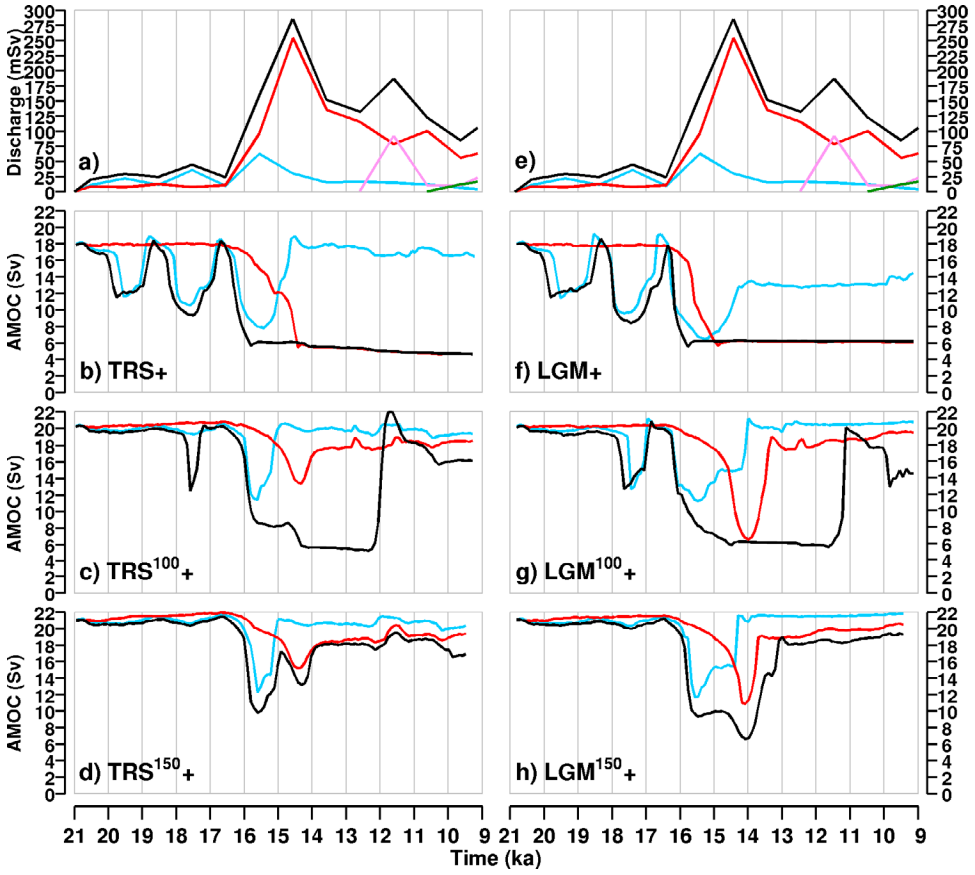

Figure 7. Response in AMOC strength to meltwater discharges from the Fennoscandian ice sheet (blue), Laurentide ice sheet (red) and all ice sheets (black) for (left) a transient background climate and (right) a constant 21 ka background climate. (a, e) Meltwater discharge rate (mSv), (b, f) AMOC response (Sv) in high sensitivity, (c, g) medium sensitivity, and (d, h) low sensitivity model configuration. Discharge rates for AIS (pink) and GIS (green) are shown for reference as they contribute to the total meltwater forcing.

the 9 ka overturning circulation continues its gradual decrease for 50 mSv of additional forcing, at which point it undergoes a two-step collapse that is complete by 250 mSv. The single step collapse in HYS^{21ka} is consistent with the presence of only one deep-water formation site in the North Atlantic; the two step behavior in HYS^{9ka} indicates a preliminary shift of the deep-water formation from the northwest Atlantic to the Nordic Seas before the collapse occurs. In the "off" (lower) branch of the hysteresis curves, the overturning maintains a relatively constant strength (~5 Sv, with HYS^{21ka} being slightly stronger than HYS^{9ka}) as the freshwater forcing is reduced. A negative freshwater flux of 50–60 mSv is needed to bring the AMOC back to the stable regime, although we cannot exclude the possibility that freshwater input to the Southern Ocean could facilitate the AMOC resumption. The resumption is followed by a small 2–4 Sv overshoot in both background climate states.

[35] An important feature of the stable branch is that the slopes are slightly curved, meaning that the sensitivity is not entirely linear and increases as the freshwater forcing increases. In particular, in the monostable regime (i.e., <−50 mSv) the sensitivity is rather flat, a feature that has implications for the response to small meltwater inputs in our reduced sensitivity simulations. The curvature itself is an indication of Stommel's salt advection feedback while the abrupt collapse points to the dominant role of convective instability in the model [*Rahmstorf et al.*, 2005].

[36] It should be noted that the AMOC behavior in these hysteresis experiments does not exactly reflect the model sensitivity to meltwater from LIS and FIS due to the dependence of the AMOC response on the rate of change and location of freshwater input. Hysteresis experiments, in which freshwater is applied over a broad region from 20–50°N, generally underestimate the model sensitivity to high northern meltwater inputs, which have a more direct impact on convection sites and are less easily evacuated [*Mignot et al.*, 2007; *Smith and Gregory*, 2009; *Roche et al.*, 2010]. Nevertheless, the experiments provide a useful framework for the discussion in the next two sections.

4.2. Effect of Uncertainties in the Model Sensitivity

[37] The meltwater forcing and AMOC response for the baseline simulation TRS+ALL are shown in Figures 7a and 7b (black curves). In this default model configuration, the AMOC collapses partway through the deglaciation (16 ka) and never recovers, an outcome that is clearly unrealistic. Assuming that the freshwater forcing scenario is reasonable, this result suggests that the model is overly sensitive to freshwater input.

[38] To evaluate the effect of uncertainty in the freshwater sensitivity of the model, we perform two additional experiments with reduced AMOC sensitivity. As shown in the previous section, the IGSM2 exhibits hysteresis behavior within range of the models in the *Rahmstorf et al.* [2005] intercomparison study, but its recovery (left) branch sits slightly to the "left" in freshwater flux space [*Rahmstorf et al.*, 2005, Figure 2]. In the reduced sensitivity experiments we apply constant freshwater fluxes of −100 mSv (TRS100+) and −150 mSv (TRS150+) to the latitudinal band 20–50°N of the Atlantic, effectively shifting the hysteresis curves to the right, with the new zero freshwater flux lines indicated by dashed grey lines in Figure 6. The sensitivity to small meltwater inputs is somewhat reduced since the shift moves the portion of the hysteresis curve with gentler slopes closer to the zero freshwater flux line. More importantly, the shift means that a shutdown is less easily achieved, and the resumption threshold is shifted to the positive freshwater flux sector of the hysteresis diagram.

[39] Figure 7 (left) shows a comparison of the AMOC response for all three sensitivity cases. The response in the reduced sensitivity scenarios (Figures 7c and 7d) is strongly damped compared to the baseline scenarios (Figure 7b). For example, with reduced sensitivity, the first two FIS pulses have virtually no effect, whether alone (blue curves showing simulations (Figure 7c) TRS^{100}+FIS and (Figure 7d) TRS^{150}+FIS) or in combination with the other ice sheet discharges (black curves showing simulations (Figure 7c) TRS^{100}+ALL and (Figure 7d) TRS^{150}+ALL).

[40] Along the lines of the discussion in section 4.1, some interesting nonlinear effects become apparent in comparing the three sensitivity cases, especially when the separate meltwater contributions from FIS (blue curves) and LIS (red curves) are considered. The AMOC collapses around 16 ka in the baseline TRS+ALL simulation (Figure 7b, black curve) due to a combination of FIS and LIS discharges, although the LIS discharge alone in TRS+LIS also causes a collapse delayed by about 1500 years (Figure 7b, red curve). With slightly reduced freshwater sensitivity (TRS^{100}+ALL), the combined LIS and FIS contribution around 16 ka still results in a circulation collapse (Figure 7c, black curve), but the LIS contribution in TRS^{100}+LIS alone causes only a minor AMOC weakening (Figure 7c, red curve, ∼14 ka) that is even smaller than the weakening associated with the third FIS pulse in TRS^{100}+FIS (Figure 7c, blue curve, 15–16 ka). In the case with the lowest sensitivity (TRS^{150}+ALL), the AMOC response is even weaker and no shutdown is triggered (Figure 7d, black curve).

[41] In the reduced sensitivity scenario TRS^{100}+ALL, an AMOC resumption is simulated toward the end of the deglaciation (Figure 7c, black curve, ∼12 ka). This resumption is possibly facilitated by AIS meltwater (Figure 7a, pink curve), but the reduction in meltwater input from LIS and FIS around ∼12 ka could alone be sufficient to trigger the resumption (the hysteresis diagram suggests a threshold of ∼50 mSv). The AMOC overshoot of 2 Sv following the resumption (Figure 7c, black curve, ∼12 ka) has no significant effect on NH temperatures (not shown). Close to the end of the deglaciation, a small GIS contribution of less than 25 mSv (Figure 7a, green curve) noticeably enhances the AMOC response.

[42] This set of experiments illustrates that altering the freshwater sensitivity of a model, or more specifically, shifting its AMOC hysteresis curve, can yield different outcomes for the deglaciation, from cases where the AMOC collapses completely and irreversibly to cases where the AMOC oscillates between stronger and weaker periods. The results presented here also point to the fact that the response is determined by a complex interplay of meltwater from different source regions entering the system under different background states.

4.3. Effect of a Transient Background Climate

[43] Previous studies described in the introduction have shown that the simulated response to freshwater and the recovery from a freshening event can be different in different background climates. The simulations described in the previous section, although not designed to explicitly test this question, support this result. The background climate, and thus the hysteresis behavior of the model, change through the course of the deglaciation, so a given freshwater input could produce the wrong climate response if it is introduced to the system at the wrong time. To investigate this idea, we use the same 21–9 ka meltwater scenarios as in the previous section (FIS, LIS, and ALL), but apply them to a constant LGM (21 ka) background climate throughout the simulation (equivalently, we fix the hysteresis behavior at 21 ka). The difference in background climate between the transient (Figure 7, left) and fixed (Figure 7, right) background simulations is by construction zero at 21 ka and reaches its maximum by the end of the deglaciation.

[44] The time evolution of the climate response shows remarkable differences in the two sets of experiments. Meltwater pulses still freshen the surface (not shown) and weaken overturning in the fixed background experiments, but the response is stronger than in the equivalent transient background experiments. Contrasting LGM+FIS (Figure 7f, blue curve) with TRS+FIS (Figure 7b, blue curve), for example, the difference in the AMOC response increases with each successive Fennoscandian pulse. For the TRS^{100}+ scenarios, it is now apparent that the small response to LIS meltwater compared to FIS meltwater is indeed primarily due to the meltwater timing relative to the background climate evolution (Figures 7c versus 7g). Consistent with the hysteresis curves (Figure 6), the simulated resumption of the AMOC occurs slightly earlier in LGM^{100}+ALL (Figure 7g, black curve) than in TRS^{100}+ALL (Figure 7c, black curve) and has a less pronounced overshoot. Whether this is the case for the real ocean is uncertain, but the result illustrates how idealized hysteresis experiments may be useful for understanding more complex transient climate simulations. The enhanced AMOC sensitivity under a fixed LGM background climate is also reflected in the surface ocean conditions, with stronger interhemispheric SST differences in response to NH meltwater pulses compared to the transient background experiments (not shown).

4.4. Section Summary

[45] The simulation results presented in this section illustrate that changes in the model sensitivity to freshwater (within the range of sensitivities reported for current climate models), can have a large impact on climate evolution in deglacial simulations. Reduced AMOC sensitivity (i.e., a

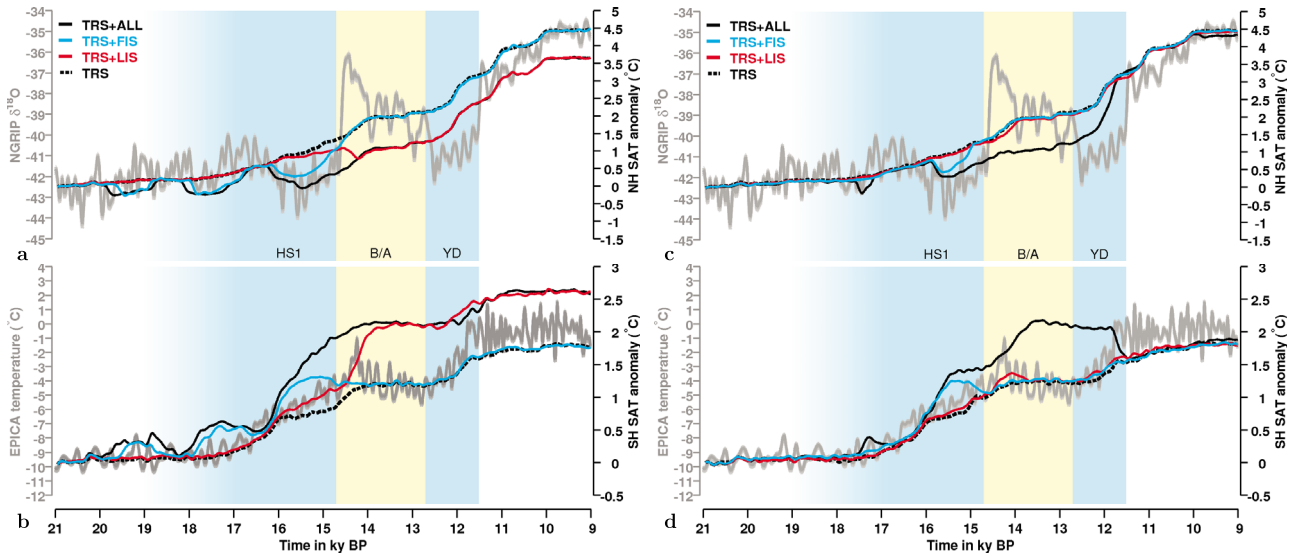

Figure 8. Hemispheric SAT response for (a, c) NH and (b, d) SH in (left) TRS+ and (right) TRS^{100}+. The dashed black line shows the response to combined orbital, ice sheet area and greenhouse gas forcings. The solid blue, red and black lines show the transient response including meltwater forcing from FIS, LIS and all ice sheets, respectively. The grey curves show δ^{18}O from the NGRIP Greenland ice core (top) and the deuterium-based temperature reconstruction from the EPICA Antarctic ice core (bottom) [*Jouzel et al.*, 2007].

more stable ocean circulation) leads to a damped response, and more importantly, may inhibit AMOC shutdowns and facilitate AMOC resumptions.

[46] In a transient framework, there is the additional complication that the AMOC sensitivity is non-stationary, with the model overturning becoming monotonically more stable during the course of the deglaciation. AMOC hysteresis experiments, while idealized, are shown to be useful for gaining insight into simulations that include complex, transient meltwater forcing. Overall, the results highlight the important role of uncertainties in model sensitivity to freshwater inputs, and additionally, of uncertainties in the meltwater history, when simulating the deglaciation.

5. Discussion

[47] We have demonstrated how uncertainties in the climate sensitivity to freshwater forcing can impact the outcome of simulations that are forced with transient meltwater histories. We used the deglaciation as our case study since the inherently nonlinear nature of the climate response to meltwater, which is shaped by nonlinear feedbacks and thresholds in the system, makes a general quantification of uncertainties (e.g., using linear error propagation theory) impracticable. Furthermore, we showed that the timing of meltwater can be decisive in a transient background climate where the freshwater sensitivity is nonstationary. In this section we discuss the implications of uncertainties in meltwater and sensitivity constraints for simulating the deglaciation.

[48] A simple comparison between our simulations and the available ice core data is a useful starting point for our discussion. Figure 8 shows the simulated hemispheric mean SAT in TRS+FIS, TRS+LIS and TRS+ALL plotted against the δ^{18}O record from the Greenland NGRIP ice core [*Johnsen et al.*, 2001] and deuterium-based temperature reconstruction from the Antarctic EPICA ice core [*Jouzel et al.*, 2007]. Antarctic temperature variability is representative of hemispheric to global scale changes [*Masson-Delmotte et al.*, 2006; *Singarayer and Valdes*, 2010], whereas Greenland variability reflects regional changes in parameters such as local temperature, precipitation, and sea ice cover [*Masson-Delmotte et al.*, 2005; *Li et al.*, 2005, 2010]. Thus, the NGRIP record is not expected to match the simulated NH SAT, particularly given the zonally averaged nature of our atmosphere model, but rather is used as a visual reference. In general, including freshwater forcing from melting ice sheets enhances millennial-scale variability in hemispheric SAT, but does not produce a good match to the millennial-scale variability in the proxy record. In the NH (Figure 8a), meltwater-driven variability (difference between TRS+ simulations and baseline TRS simulation) in the early part of the deglaciation (21–16 ka) is controlled by Fennoscandian meltwater pulses, while the Laurentide contribution becomes important after 15.5 ka. Although we do not expect a faithful reproduction of the ice core records from our model, the exercise of comparing the simulation to the data highlights the complexity of trying to link features of the observed record to features of the forcing. For example, the model captures part of the NH cooling during the later part of Heinrich Stadial 1 (HS1, 18–15 ka); however, the simulated cooling is a result of a FIS meltwater pulse amplified by a minor LIS contribution (totaling ~3.5 m sea level equivalent), while Heinrich stadials are associated with episodes of LIS iceberg discharges into the North Atlantic (known as Heinrich events). Conversely, the Bølling-Allerød (BA) warming at ~15 ka is not captured by the model (we return to this point shortly), and our simulated cold state during and after mwp1a (~14.5 ka) is inconsistent with the Greenland ice core record (the possibility that an

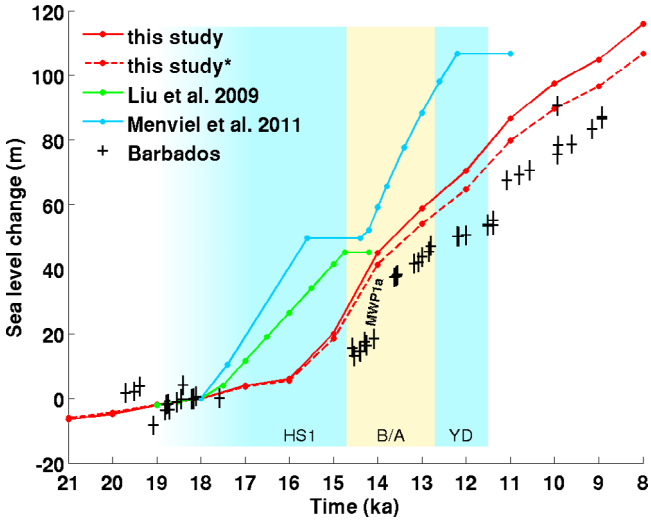

Figure 9. Accumulated freshwater discharge versus Barbardos sea level data. Red solid curve shows the sea level change corresponding to our ALL meltwater scenario, while the dashed curve uses a more accurate ice density of ρ_{ice} = 920 kg m^{-3}. The green and blue curves show the sea level changes corresponding to the freshwater scenarios used by *Liu et al.* [2009] and *Menviel et al.* [2011], respectively. The uplift corrected Barbados coral record [*Peltier and Fairbanks*, 2006] based on the single species Acropora Palmata is shown with black crosses. For the conversion of freshwater fluxes to equivalent global sea level changes, a contemporary, fixed ocean fraction of 71% has been assumed. All changes are relative to 18 ka.

incorrect NH-SH partitioning of mwp1a is responsible for the lack of a Greenland response during this time is however under debate [*Clark et al.*, 1996; *Weaver et al.*, 2003; *Peltier*, 2005; *Menviel et al.*, 2011]). The simulated AMOC also compares unfavorably with estimates from the proxy record. The ^{231}Pa/^{230}Th proxy suggests a strong overturning circulation at LGM, a collapse during the beginning of HS1, and recovery during the BA warming [*McManus et al.*, 2004]. However, the simulated AMOC (Figure 7b) collapses 2 ky later than the "Heinrich" meltwater pulse and fails to recover at the end of HS1.

[49] Although not a focus of this study, the large uncertainties in the amount, timing, shape and location of the discharge pulses in the deglacial meltwater history are part of the reason why simulating the deglaciation is so difficult. For ice sheet reconstructions based on isostasy, there are large differences in details (not shown) between the recent products ICE-4G, ICE-5G (used in the this study) and the newly released ICE-6G [*Peltier*, 2004; *Peltier and Fairbanks*, 2006; *Argus and Peltier*, 2010]. Coastal uplift rates derived from radiocarbon dated shoreline indicators help to constrain the reconstructions, but are subject to considerable spatio-temporal uncertainties that limit the temporal resolution needed to pin down abrupt events (e.g., Heinrich Event 1 at ~17.5 ka [*Dowdeswell et al.*, 1995], with a duration that could be as short as 250 years [*MacAyeal*, 1993]). We return to the example of the HS1/BA transition, which is not well simulated by IGSM2 under a meltwater forcing scenario based on ICE-5G, but which has been simulated in other modeling studies under hypothetical meltwater scenarios [*Liu et al.*, 2009; *Menviel et al.*, 2011]. Figure 9 shows the accumulated global meltwater discharges for three scenarios together with the calibrated Barbados coral record for global sea level change. Our scenario, with small amounts (<20 m) of meltwater during HS1 and a continuation of LIS discharge at the end of HS1 as implied by ICE-5G (Figure 1b), is in line with the sea level curve where coral data is available but results in no apparent BA warming. The *Liu et al.* [2009] and *Menviel et al.* [2011] scenarios generate and maintain the cold HS1 via large inputs of meltwater to the ocean (40–50 m sea level equivalent), and produce the BA warming via an AMOC resumption and overshoot triggered by the abrupt cessation of LIS discharge at the end of HS1. These studies achieved their aim of producing a deglacial AMOC history that is consistent with the paleoproxy records by scaling the meltwater forcing to compensate for deficiencies in model sensitivity and meltwater representation (a point that we will return to later in this section). The fact that sea level data do not take into account hidden meltwater contributions from floating ice shelves or processes such as ice sheet regrowth [*Rinterknecht et al.*, 2006] provide substantial leeway for adjusting meltwater scenarios.

[50] Did we succeed in obtaining a better fit with the proxy record by tuning the freshwater sensitivity of our model? A comparison of hemispheric SAT from TRS^{100}+ with ice core proxy data from Greenland and Antarctica (Figures 8c and 8d) suggests that we did not. With reduced AMOC sensitivity, the BA warming is still absent in the NH average. The simulated response is closer to the proxy record during the cold Younger Dryas (12.7–11.5 ka) period, but the shutdown is triggered during mwp1a and not as a consequence of a later meltwater input as suggested by some studies [e.g., *Tarasov and Peltier*, 2005, 2006]. The small response to the LIS contribution to mwp1a includes a slight cooling in the NH (Figure 8c, red curve) that coincides approximately with the Older Dryas (~14 ka), and a SH warming (Figure 8d, red curve) that may contribute to the shape of the Antarctic Cold Reversal (~14.5–12.5 ka). Thus, under a range of different model sensitivities, the implied ICE-5G meltwater partitioning fails to produce key features of the deglaciation.

[51] Along with general uncertainties in meltwater forcing and climate sensitivity to meltwater, the non-stationarity of the sensitivity (i.e., increasing AMOC stability as the background climate warms) is an additional consideration. The enhanced AMOC stability in the present climate compared to the glacial climate has been attributed to deglacial Southern Ocean warming in combination with increased salt import to the Atlantic from the Indian Ocean [*Knorr and Lohmann*, 2003]; the Bering Strait pathway for evacuating freshwater anomalies from the North Atlantic [*De Boer and Nof*, 2004a, 2004b; *Hu et al.*, 2007]; and retreat of the sea ice edge with respect to convection areas [*Bitz et al.*, 2007]. In our model, ice edge retreat is the most likely candidate since subtle changes in Southern Ocean winds, Atlantic-Indian Ocean exchanges and bathymetry are not resolved or included. While it is possible that shifts in ocean circulation alter model sensitivity to meltwater at critical times during the deglaciation (e.g., close to the BA warming), this topic is beyond the scope of this study. Another interesting issue is how the transient meltwater forcing interacts with the

transient background climate. Most idealized hosing studies show a complete recovery of the overturning strength in less than 1 ky [e.g., *Liu et al.*, 2009, Figure S7], but ocean ventilation ages of several ky in proxy and model data [*Okazaki et al.*, 2010] indicate that the deep ocean memory to freshwater forcing is considerably longer. The main implication of the results presented here is that errors in meltwater timing have a complex, nonlinear impact on the climate response in changing background conditions.

[52] Many challenges remain in combining data constraints and modeling experiments to better understand the last deglaciation. There are benefits to be gained by improving meltwater constraints, such as establishing more clearly the effect of meltwater contributions from non-Laurentide sources early in the deglaciation. But even a "perfect" meltwater scenario may produce a simulated deglaciation that differs from the proxy record as long as model uncertainties in freshwater sensitivity remain large [*Rahmstorf et al.*, 2005; *Stouffer et al.*, 2006] and the possible role of other (i.e., non-meltwater) processes is not included [e.g., *Eisenman et al.*, 2009]. However, reducing the uncertainty in model sensitivities is a demanding task due to the nonlinearity of the climate response to meltwater, the need to consider transient background climates, the cost of running high-resolution models over longer time periods, and not least the sparseness of proxy data.

[53] One fruitful approach may be to use improved meltwater constraints provided by proxy data and by ice sheet models to test proposed mechanisms concerning specific events in the climate record, with the forcings scaled to compensate for deficiencies such as the uncertainty in model sensitivity [e.g., *Smith and Gregory*, 2009]. Otherwise, it may be possible to extend forward-modeling from a deterministic to a probabilistic approach by using multimodel and multiforcing ensembles to span the range of plausible model sensitivities and meltwater forcings. Inverse approaches such as the one used by *Menviel et al.* [2011] have shown potential, although they tend to conceal the effects of processes not represented by the model [*Adkins et al.*, 2005; *Wunsch*, 2005] and of model deficiencies. The next step would be to use more sophisticated and objective assimilation methods for proxy data [e.g., *Gebbie and Huybers*, 2006; *Huybers et al.*, 2007; *Dail et al.*, 2010; *Jackson et al.*, 2010].

[54] Our study has certain caveats. The model system is too simplistic to resolve sea ice atmospheric circulation feedbacks [*Li et al.*, 2010] and other important processes that may shape glacial climate variability, such as the impact of ice sheet topography on atmospheric circulation patterns [*Pausata et al.*, 2009, 2011]. Hence, our simulated climate variability might be overly connected to ocean overturning variability, with the role of the atmosphere underestimated. In particular, the simulations of *Eisenman et al.* [2009] exhibit AMOC variability linked to changes in North Atlantic precipitation as ice sheets recede. The link between sea ice and AMOC sensitivity is still debated; while our model and others [e.g., *Bitz et al.*, 2007] indicate that sea ice retreat has a stabilizing effect, others show the opposite result [*Van Meerbeeck et al.*, 2011]. The virtual salt flux [*Yin et al.*, 2010] and flux-adjustments [*Shackley et al.*, 1999] in our model introduce further uncertainties, especially in climates that are very different from today's climate or that experience large meltwater inputs. Finally, the Bering Strait is open during the entire simulation, whereas in reality, it was closed until at least 11 ka [*Elias et al.*, 1997]. Previous studies have shown that an open Bering Strait can provide an evacuation pathway for the North Atlantic freshwater anomalies, thus helping to stabilize the overturning circulation [*De Boer and Nof*, 2004a, 2004b; *Hu and Meehl*, 2005; *Hu et al.*, 2007]. A simulated weakening of the Bering Strait throughflow after meltwater pulses enter the North Atlantic suggest that this pathway also exists in IGSM2.

6. Concluding Remarks

[55] We have performed a series of transient simulations of the last deglaciation (21–9 ka) to explore the extent to which deglacial climate variability is driven by freshwater discharges from melting ice sheets and to assess whether ice sheet reconstructions can provide meltwater constraints in deglacial simulations. Using an objectively constructed meltwater history based solely on the ICE-5G ice sheet reconstruction, we demonstrate the importance of the volume, timing and location of meltwater inputs to the ocean, as well as the inadequacy of current data constraints on these parameters. We show how the simulated deglacial evolution differs in model configurations with different freshwater sensitivities. Finally, we assess the role of a transient background climate by comparing the effect of meltwater pulses in fully transient simulations to the effect in simulations with a fixed, 21 ka background climate.

[56] The main findings of this work are as follows.

[57] 1. The temporal evolution of the climate response to NH meltwater discharges bears little resemblance to the meltwater forcing itself, but is similar among key climate variables such as sea ice extent, North Atlantic sea surface salinity and ocean overturning strength. Positive feedback processes are important in shaping the response. The nonlinearity of the climate response to meltwater makes it difficult to tie features in the proxy record to specific meltwater pulses.

[58] 2. Simulations using model configurations with altered freshwater sensitivity suggest that different models would produce a considerable range of outcomes for the deglaciation given the same meltwater forcing history. The proximity of the system to circulation thresholds at any given time during the simulated deglaciation is found to be decisive, whereas uncertainties in the approximately linear sensitivity to modest meltwater inputs have a modulating effect. Idealized hysteresis experiments prove useful for interpreting the climate response to complex meltwater histories under a changing background climate.

[59] 3. The climate sensitivity to meltwater inputs depends on the changing background climate. Consequently, errors in the timing of meltwater pulses have an important, and not easily predictable, impact on the climate response: a given pulse in a history of pulses may cause a weakening or collapse of the AMOC if introduced to different backgrounds. In our model, the decrease in sensitivity is likely linked to the gradual sea ice retreat and northward migration of the overturning circulation into the Nordic Seas as the slow (greenhouse gas, ice sheet extent, orbital) forcings change through the course of deglaciation.

[60] To return to the title question, it is unlikely that a forward modeling approach using objectively derived, "best-guess" meltwater histories based on data reconstructions will faithfully reproduce the deglaciation. The main impediments are (1) uncertainties in the meltwater history, (2) uncertainties in the model sensitivity to freshwater forcing, and (3) the role of nonlinear feedback processes in shaping the response and potentially amplifying the uncertainties. Thus, implied meltwater rates from ice sheet reconstructions cannot be readily used like other forcings to constrain deglacial simulations. Moreover, other processes not controlled by meltwater may still be important for producing deglacial climate variability.

[61] This and previous simulation studies [*Liu et al.*, 2009; *Menviel et al.*, 2011] have shown that meltwater can play an important role in shaping millennial scale climate variability during the deglaciation. Improving constraints on the amount, timing and location of freshwater inputs to the ocean and reducing uncertainties in model sensitivity to meltwater are important tasks. Further studies with more complex models and more realistic experimental setups (e.g., including effects from orographic and sea level changes) are required to test the robustness of the findings presented here.

[62] **Acknowledgments.** We wish to thank Bjørg Risebrobakken, Odd Helge Otterå, Didier Roche, Axel Timmermann, and one anonymous reviewer for helpful discussion and comments. This is publication A394 from the Bjerknes Centre for Climate Research, funded by the ARCTREC project.

References

Adkins, J., A. Ingersoll, and C. Pasquero (2005), Rapid climate change and conditional instability of the glacial deep ocean from the thermobaric effect and geothermal heating, *Quat. Sci. Rev.*, *24*(5–6), 581–594.

Alley, R. (2000), The Younger Dryas cold interval as viewed from central Greenland, *Quat. Sci. Rev.*, *19*(1–5), 213–226.

Alley, R., and P. Clark (1999), The deglaciation of the northern hemisphere: a global perspective, *Annu. Rev. Earth Planet. Sci.*, *27*(1), 149–182.

Argus, D., and W. Peltier (2010), Constraining models of postglacial rebound using space geodesy: A detailed assessment of model ice-5g (vm2) and its relatives, *Geophys. J. Int.*, *181*(2), 697–723.

Berger, A. (1978), Long-term variations of caloric insolation resulting from the earth's orbital elements, *Quat. Res.*, *9*(2), 139–167.

Bitz, C., and W. Lipscomb (1999), An energy-conserving thermodynamic model of sea ice, *J. Geophys. Res.*, *104*(15), 15,669–15,677.

Bitz, C., M. Holland, E. Hunke, and R. Moritz (2005), Maintenance of the sea-ice edge, *J. Clim.*, *18*, 2903–2921.

Bitz, C., J. Chiang, W. Cheng, and J. Barsugli (2007), Rates of thermohaline recovery from freshwater pulses in modern, Last Glacial Maximum, and greenhouse warming climates, *Geophys. Res. Lett.*, *34*, L07708, doi:10.1029/2006GL029237.

Boyle, E. A., and L. Keigwin (1987), North Atlantic thermohaline circulation during the past 20,000 years linked to high-latitude surface temperature, *Nature*, *330*(6143), 35–40.

Braconnot, P., et al. (2004), Evaluation of PMIP coupled ocean-atmosphere simulations of the Mid-Holocene, in *Past Climate Variability Through Europe and Africa*, edited by R. W. Battarbee, F. Gasse, and C. E. Stickley, pp. 515–533, Springer, Dordrecht, Netherlands.

Braconnot, P., et al. (2007), Results of PMIP2 coupled simulations of the Mid-Holocene and Last Glacial Maximum–Part 1: experiments and large-scale features, *Clim. Past*, *3*(2), 261–277.

Broccoli, A., and S. Manabe (1987), The influence of continental ice, atmospheric CO_2, and land albedo on the climate of the last glacial maximum, *Clim. Dyn.*, *1*(2), 87–99.

Broecker, W. (1998), Paleocean circulation during the last deglaciation: A bipolar seesaw?, *Paleoceanography*, *13*(2), 119–121.

Bush, A., and S. Philander (1999), The climate of the Last Glacial Maximum- Results from a coupled atmosphere-ocean general circulation model, *J. Geophys. Res.*, *104*(D20), 24,509–24,525.

Carlson, A. (2009), Geochemical constraints on the Laurentide Ice Sheet contribution to Meltwater Pulse 1A, *Quat. Sci. Rev.*, *28*(17–18), 1625–1630.

Cheng, W., C. M. Bitz, and J. C. H. Chiang (2007), Adjustment of the global climate to an abrupt slowdown of the Atlantic meridional overturning circulation, in *Ocean Circulation: Mechanisms and Impacts—–Past and Future Changes of Meridional Overturning*, *Geophys. Monogr. Ser.*, vol. 173, edited by A. Schmittner, J. C. H. Chiang, and S. R. Hemming, pp. 295–313, AGU, Washington, D. C., doi:10.1029/173GM19.

Clark, P., and A. Mix (2001), Ice sheets and sea level of the Last Glacial Maximum, *Quat. Sci. Rev.*, *21*(1–3), 1–7.

Clark, P., R. Alley, L. Keigwin, J. Licciardi, S. Johnsen, and H. Wang (1996), Origin of the first global meltwater pulse following the last glacial maximum, *Paleoceanography*, *11*(5), 563–577.

Clark, P., S. Marshall, G. Clarke, S. Hostetler, J. Licciardi, and J. Teller (2001), Freshwater forcing of abrupt climate change during the last glaciation, *Science*, *293*(5528), 283–287.

Clark, P., J. Mitrovica, G. Milne, and M. Tamisiea (2002), Sea-level fingerprinting as a direct test for the source of global meltwater pulse IA, *Science*, *295*(5564), 2438–2441.

Claussen, M., et al. (2002), Earth system models of intermediate complexity: closing the gap in the spectrum of climate system models, *Clim. Dyn.*, *18*(7), 579–586.

Crowley, T. (1992), North Atlantic Deep Water cools the southern hemisphere, *Paleoceanography*, *7*, 489–497.

Crowley, T., and S. Baum (1997), Effect of vegetation on an ice-age climate model simulation, *J. Geophys. Res.*, *102*(D14), 16,463–16,480.

Curry, W., and D. Oppo (2005), Glacial water mass geometry and the distribution of $\delta^{13}C$ of $\sum CO_2$ in the western Atlantic Ocean, *Paleoceanography*, *20*, PA1017, doi:10.1029/2004PA001021.

Dail, H., P. Heimbach, and C. Wunsch (2010), State estimation of atlantic ocean circulation at the last glacial maximum, *Geophys. Res. Abstr.*, *12*, 5664.

De Boer, A., and D. Nof (2004a), The exhaust valve of the North Atlantic, *J. Clim.*, *17*(3), 417–422.

De Boer, A., and D. Nof (2004b), The bering strait's grip on the northern hemisphere climate, *Deep Sea Res., Part I*, *51*(10), 1347–1366.

Dong, B., and P. Valdes (1998), Simulations of the Last Glacial Maximum climates using a general circulation model: Prescribed versus computed sea surface temperatures, *Clim. Dyn.*, *14*(7–8), 571–591.

Dowdeswell, J., M. Maslin, J. Andrews, and I. McCave (1995), Iceberg production, debris rafting, and the extent and thickness of Heinrich layers (H-1, H-2) in North Atlantic sediments, *Geology*, *23*(4), 301–304.

Duplessy, J., N. Shackleton, R. Fairbanks, L. Labeyrie, D. Oppo, and N. Kallel (1988), Deepwater source variations during the last climatic cycle and their impact on the global deepwater circulation, *Paleoceanography*, *3*(3), 343–360.

Dutkiewicz, S., A. Sokolov, J. Scott, and P. Stone (2005), A three-dimensional ocean-seaice-carbon cycle model and its coupling to a two-dimensional atmospheric model: Uses in climate change studies, *Rep. 122*, Joint Program on the Sci. and Policy of Global Change, Mass. Inst. of Technol., Cambridge.

Eisenman, I., C. Bitz, and E. Tziperman (2009), Rain driven by receding ice sheets as a cause of past climate change, *Paleoceanography*, *24*, PA4209, doi:10.1029/2009PA001778.

Elias, S., S. Short, and H. Birks (1997), Late Wisconsin environments of the Bering Land Bridge, *PPalaeogeogr. Palaeoclimatol. Palaeoecol.*, *136*, 293–308.

Fairbanks, R. (1989), A 17,000-year glacio-eustatic sea level record: influence of glacial melting rates on the Younger Dryas event and deep-ocean circulation, *Nature*, *342*, 637–642.

Ganopolski, A. and S. Rahmstorf (2001), Rapid changes of glacial climate simulated in a coupled climate model, *Nature*, *409*(6817), 153–158.

Ganopolski, A., S. Rahmstorf, V. Petoukhov, and M. Claussen (1998), Simulation of modern and glacial climates with a coupled global model of intermediate complexity, *Nature*, *391*(6665), 351–356.

Gebbie, G., and P. Huybers (2006), Meridional circulation during the last glacial maximum explored through a combination of south atlantic $\delta^{18}O$ observations and a geostrophic inverse model, *Geochem. Geophys. Geosyst.*, *7*, Q11N07, doi:10.1029/2006GC001383.

Hewitt, C., A. Broccoli, J. Mitchell, and R. Stouffer (2001), A coupled model study of the last glacial maximum: Was part of the North Atlantic relatively warm?, *Geophys. Res. Lett.*, *28*(8), 1571–1574.

Hofmann, M., and S. Rahmstorf (2009), On the stability of the atlantic meridional overturning circulation, *Proc. Natl. Acad. Sci. U. S. A.*, *106*(49), 20,584–20,589.

Hu, A., and G. Meehl (2005), Bering Strait throughflow and the thermohaline circulation, *Geophys. Res. Lett*, *32*, 859–862.

Hu, A., G. Meehl, and W. Han (2007), Role of the Bering Strait in the thermohaline circulation and abrupt climate change, *Geophys. Res. Lett.*, *34*, L24610, doi:10.1029/2005GL024424.

Hu, A., B. Otto-Bliesner, G. Meehl, W. Han, C. Morrill, E. Brady, and B. Briegleb (2008), Response of thermohaline circulation to freshwater forcing under present-day and LGM conditions, *J. Clim.*, *21*(10), 2239–2258.

Huybers, P., G. Gebbie, and O. Marchal (2007), Can paleoceanographic tracers constrain meridional circulation rates?, *J. Phys. Oceanogr.*, *37*(2), 394–407.

Lambeck, K., Y. Yokoyama, and T. Purcell (2002), Into and out of the Last Glacial Maximum: Sea-level change during Oxygen Isotope Stages 3 and 2, *Quat. Sci. Rev.*, *21*(1–3), 343–360.

Jackson, C., O. Marchal, Y. Liu, S. Lu, and W. Thompson (2010), A box model test of the freshwater forcing hypothesis of abrupt climate change and the physics governing ocean stability, *Paleoceanography*, *25*, PA4222, doi:10.1029/2010PA001936.

Jansen, E., et al. (2007), Paleoclimate, in *Climate Change 2007: The Physical Science Basis. Contribution of Working Group I to the Fourth Assessment Report of the Intergovernmental Panel on Climate Change*, edited by S. Solomon et al., pp. 433–497, Cambridge Univ. Press, New York.

Johnsen, S., D. Dahl-Jensen, N. Gundestrup, J. Steffensen, H. Clausen, H. Miller, V. Masson-Delmotte, A. Sveinbjörnsdottir, and J. White (2001), Oxygen isotope and palaeotemperature records from six Greenland ice-core stations: Camp Century, Dye-3, GRIP, GISP2, Renland and NorthGRIP, *J. Quat. Sci.*, *16*(4), 299–307.

Jouzel, J., et al. (2007), Orbital and millennial Antarctic climate variability over the past 800,000 years, *Science*, *317*(5839), 793–797.

Justino, F., A. Timmermann, U. Merkel, and E. Souza (2005), Synoptic Reorganization of Atmospheric Flow during the Last Glacial Maximum, *J. Clim.*, *18*(15), 2826–2846.

Knorr, G., and G. Lohmann (2003), Southern Ocean origin for the resumption of Atlantic thermohaline circulation during deglaciation, *Nature*, *424*(6948), 532–536.

Knutti, R., J. Flückiger, T. Stocker, and A. Timmermann (2004), Strong hemispheric coupling of glacial climate through freshwater discharge and ocean circulation, *Nature*, *430*(7002), 851–856.

Krebs, U. and A. Timmermann (2007), Tropical air-sea interactions accelerate the recovery of the Atlantic meridional overturning circulation after a major shutdown, *J. Clim.*, *20*(19), 4940–4956.

Langen, P. L., and B. M. Vinther (2009), Response in atmospheric circulation and sources of Greenland precipitation to glacial boundary conditions, *Clim. Dyn.*, *32*, 1035–1054.

Li, C., D. Battisti, D. Schrag, and E. Tziperman (2005), Abrupt climate shifts in Greenland due to displacements of the sea ice edge, *Geophys. Res. Lett.*, *32*, L19702, doi:10.1029/2005GL023492.

Li, C., D. Battisti, and C. Bitz (2010), Can North Atlantic sea ice anomalies account for Dansgaard-Oeschger climate signals?, *J. Clim.*, *23*(20), 5457–5475.

Liu, Z., et al. (2009), Transient simulation of last deglaciation with a new mechanism for Bolling-Allerod warming, *Science*, *325*(5938), 310.

Lohmann, G., and S. Lorenz (2000), On the hydrological cycle under paleoclimatic conditions as derived from AGCM simulations, *J. Geophys. Res.*, *105*(17), 17,417–17,436.

Lund, D., J. Adkins, and R. Ferrari (2011), Abyssal Atlantic circulation during the Last Glacial Maximum: Constraining the ratio between transport and vertical mixing, *Paleoceanography*, *26*, PA1213, doi:10.1029/2010PA001938.

Lunt, D., M. Williamson, P. Valdes, T. Lenton, and R. Marsh (2006), Comparing transient, accelerated, and equilibrium simulations of the last 30,000 years with the GENIE-1 model, *Clim. Past*, *2*(2), 221–235.

MacAyeal, D. (1993), A low-order model of the Heinrich Event Cycle, *Paleoceanography*, *8*(6), 767–773.

Marchitto, T., and K. Wei (1995), History of laurentide meltwater flow to the gulf of mexico during the last deglaciation, as revealed by reworked calcareous nannofossils, *Geology*, *23*(9), 779–782.

Marshall, J., A. Adcroft, C. Hill, L. Perelman, and C. Heisey (1997), A finite-volume, incompressible Navier Stokes model for studies of the ocean on parallel computers, *J. Geophys. Res.*, *102*(C3), 5753–5766.

Masson-Delmotte, V., J. Jouzel, A. Landais, M. Stievenard, S. Johnsen, J. White, M. Werner, A. Sveinbjornsdottir, and K. Fuhrer (2005), GRIP deuterium excess reveals rapid and orbital-scale changes in Greenland moisture origin, *Science*, *309*(5731), 118–121.

Masson-Delmotte, V., et al. (2006), Past and future polar amplification of climate change: climate model intercomparisons and ice-core constraints, *Clim. Dyn.*, *26*(5), 513–529.

McManus, J., R. Francois, J. Gherardi, L. Keigwin, and S. Brown-Leger (2004), Collapse and rapid resumption of Atlantic meridional circulation linked to deglacial climate changes, *Nature*, *428*(6985), 834–837.

Medhaug, I., and T. Furevik (2011), North atlantic 20th century multidecadal variability in coupled climate models: sea surface temperature and ocean overturning circulation, *Ocean Sci. Discuss.*, *8*, 353–396.

Meehl, G., C. Covey, T. Delworth, M. Latif, B. McAvaney, J. Mitchell, R. Stouffer, and K. Taylor (2007), The WCRP CMIP3 Multimodel Dataset: A new era in climate change research, *Bull. Am. Meteorol. Soc.*, *88*, 1383–1394.

Menviel, L., A. Timmermann, O. Timm, and A. Mouchet (2011), Deconstructing the Last Glacial termination: the role of millennial and orbital-scale forcings, *Quat. Sci. Rev.*, *30*, 1155–1172.

Mignot, J., A. Ganopolski, and A. Levermann (2007), Atlantic subsurface temperatures: Response to a shutdown of the overturning circulation and consequences for its recovery, *J. Clim.*, *20*(19), 4884–4898.

Monnin, E., A. Indermuhle, A. Dallenbach, J. Fluckiger, B. Stauffer, T. Stocker, D. Raynaud, and J. Barnola (2001), Atmospheric CO_2 concentrations over the last glacial termination, *Science*, *291*(5501), 112–114.

Murton, J., M. Bateman, S. Dallimore, J. Teller, and Z. Yang (2010), Identification of Younger Dryas outburst flood path from Lake Agassiz to the Arctic Ocean, *Nature*, *464*(7289), 740–743.

Okazaki, Y., A. Timmermann, L. Menviel, N. Harada, A. Abe-Ouchi, M. Chikamoto, A. Mouchet, and H. Asahi (2010), Deepwater formation in the north pacific during the last glacial termination, *Science*, *329*(5988), 200–204.

Otto-Bliesner, B., and E. Brady (2010), The sensitivity of the climate response to the magnitude and location of freshwater forcing: last glacial maximum experiments, *Quat. Sci. Rev.*, *29*(1–2), 56–73.

Otto-Bliesner, B., C. Hewitt, T. Marchitto, E. Brady, A. Abe-Ouchi, M. Crucifix, S. Murakami, and S. Weber (2007), Last Glacial Maximum ocean thermohaline circulation: PMIP2 model intercomparisons and data constraints, *Geophys. Res. Lett.*, *34*(12), L12706, doi:10.1029/2007GL029475.

Pausata, F., C. Li, J. Wettstein, K. Nisancioglu, and D. Battisti (2009), Changes in atmospheric variability in a glacial climate and the impacts on proxy data: a model intercomparison, *Clim. Past Discuss.*, *5*, 911–936.

Pausata, F., C. Li, J. Wettstein, M. Kageyama, and K. Nisancioglu (2011), The key role of topography in altering North Atlantic atmospheric circulation during the last glacial period, *Clim. Past Discuss.*, *7*, 575–599.

Peltier, W., and R. Fairbanks (2006), Global glacial ice volume and Last Glacial Maximum duration from an extended Barbados sea level record, *Quat. Sci. Rev.*, *25*(23–24), 3322–3337.

Peltier, W. (1994), Ice-age paleotopology, *Science*, *265*, 195–201.

Peltier, W. (2004), Global glacial isostasy and the surface of the ice-age earth: The ICE-5G (VM2) model and GRACE, *Annu. Rev. Earth Planet. Sci.*, *32*, 111–149.

Peltier, W. (2005), On the hemispheric origins of meltwater pulse 1a, *Quat. Sci. Rev.*, *24*(14–15), 1655–1671.

Peltier, W. (2009), Closure of the budget of global sea level rise over the GRACE era: the importance and magnitudes of the required corrections for global glacial isostatic adjustment, *Quat. Sci. Rev.*, *28*(17–18), 1658–1674.

Perry, G., P. Duffy, and N. Miller (1996), An extended data set of river discharges for validation of general circulation models, *J. Geophys. Res.*, *101*, 21,339–21,349.

Rahmstorf, S., et al. (2005), Thermohaline circulation hysteresis: A model intercomparison, *Geophys. Res. Lett.*, *32*, L23605, doi:10.1029/2005GL023655.

Rasmussen, S., et al. (2006), A new Greenland ice core chronology for the last glacial termination, *J. Geophys. Res.*, *111*, D06102, doi:10.1029/2005JD006079.

Rind, D. (1987), Components of the ice age circulation, *J. Geophys. Res.*, *92*(D4), 4241–4281.

Rinterknecht, V., et al. (2006), The last deglaciation of the southeastern sector of the Scandinavian ice sheet, *Science*, *311*(5766), 1449–1452.

Roche, D., A. Wiersma, and H. Renssen (2010), A systematic study of the impact of freshwater pulses with respect to different geographical locations, *Clim. Dyn.*, *34*(7), 997–1013.

Roche, D., H. Renssen, D. Paillard, and G. Levavasseur (2011), Deciphering the spatio-temporal complexity of climate change of the last deglaciation: A model analysis, *Clim. Past*, *7*, 591–602.

Scott, J., A. Sokolov, P. Stone, and M. Webster (2008), Relative roles of climate sensitivity and forcing in defining the ocean circulation response to climate change, *Clim. Dyn.*, *30*(5), 441–454.

Shackley, S., J. Risbey, P. Stone, and B. Wynne (1999), Adjusting to policy expectations in climate change modeling, *Clim. Change*, *43*(2), 413–454.

Shin, S., Z. Liu, B. Otto-Bliesner, E. Brady, J. Kutzbach, and S. Harrison (2003), A simulation of the Last Glacial Maximum climate using the NCAR-CCSM, *Clim. Dyn.*, *20*(2), 127–151.

Singarayer, J., and P. Valdes (2010), High-latitude climate sensitivity to ice-sheet forcing over the last 120 kyr, *Quat. Sci. Rev.*, *29*(1–2), 43–55.

Smith, R., and J. Gregory (2009), A study of the sensitivity of ocean overturning circulation and climate to freshwater input in different regions of the North Atlantic, *Geophys. Res. Lett.*, *36*, L15701, doi:10.1029/2009GL038607.

Sokolov, A., et al. (2005), MIT integrated global system model (IGSM) version 2: model description and baseline evaluation, *Rep. 124*, Joint Program on the Sci. and Policy of Global Change, Mass. Inst. of Technol., Cambridge.

Sokolov, A., D. Kicklighter, J. Melillo, B. Felzer, C. Schlosser, and T. Cronin (2008), Consequences of considering carbon–nitrogen interactions on the feedbacks between climate and the terrestrial carbon cycle, *J. Clim.*, *21*, 3776–3796.

Sowers, T., and M. Bender (1995), Climate records covering the last deglaciation, *Science*, *269*(5221), 210–214.

Stanford, J., E. Rohling, S. Hunter, A. Roberts, S. Rasmussen, E. Bard, J. McManus, and R. Fairbanks (2006), Timing of meltwater pulse 1a and climate responses to meltwater injections, *Paleoceanography*, *21*, PA4103, doi:10.1029/2006PA001340.

Stocker, T. (1998), Climate change: the seesaw effect, *Science*, *282*(5386), 61–62.

Stocker, T., A. Timmermann, M. Renold, and O. Timm (2007), Effects of salt compensation on the climate model response in simulations of large changes of the Atlantic Meridional Overturning Circulation, *J. Clim.*, *20*, 5912–5928.

Stone, P., and M.-S. Yao (1987), Development of a two-dimensional zonally averaged statistical-dynamical model. Part II: The role of eddy momentum fluxes in the general circulation and their para- meterization, *J. Atmos. Sci.*, *44*, 3769–3786.

Stone, P., and M.-S. Yao (1990), Development of a two-dimensional zonally averaged statistical-dynamical model. Part III: The parametrization of the eddy fluxes of heat and moisture, *J. Clim.*, *3*, 726–740.

Stouffer, R., et al. (2006), Investigating the causes of the response of the thermohaline circulation to past and future climate changes, *J. Clim.*, *19*(8), 1365–1387.

Tarasov, L., and W. Peltier (2005), Arctic freshwater forcing of the Younger Dryas cold reversal, *Nature*, *435*(7042), 662–665.

Tarasov, L., and W. Peltier (2006), A calibrated deglacial drainage chronology for the North American continent: Evidence of an Arctic trigger for the Younger Dryas, *Quat. Sci. Rev.*, *25*(7–8), 659–688.

Teller, J. (1990), Meltwater and precipitation runoff to the North Atlantic, Arctic, and Gulf of Mexico from the Laurentide ice sheet and adjacent regions during the Younger Dryas, *Paleoceanography*, *5*(6), 897–905.

Timm, O., and A. Timmermann (2007), Simulation of the last 21,000 years using accelerated transient boundary conditions, *J. Clim.*, *20*, 4377–4401.

Trenberth, K., W. Large, and J. Olson (1990), The mean annual cycle in global ocean wind stress, *J. Phys. Oceanogr.*, *20*, 1742–1760.

Van Meerbeeck, C., D. Roche, and H. Renssen (2011), Assessing the sensitivity of the North Atlantic Ocean circulation to freshwater perturbation in various glacial climate states, *Clim. Dyn.*, *37*(9–10), 1909–1927.

Weaver, A., O. Saenko, P. Clark, and J. Mitrovica (2003), Meltwater pulse 1A from Antarctica as a trigger of the Bolling-Allerod warm interval, *Science*, *299*(5613), 1709–1713.

Weber, S. (2010), The utility of Earth system Models of Intermediate Complexity (EMICs), *Wiley Interdiscip. Rev.: Clim. Change*, *1*(2), 243–252.

Weber, S., and S. Drijfhout (2007), Stability of the Atlantic Meridional Overturning Circulation in the Last Glacial Maximum climate, *Geophys. Res. Lett.*, *34*, L22706, doi:10.1029/2007GL031437.

Weber, S., S. Drijfhout, A. Abe-Ouchi, M. Crucifix, M. Eby, A. Ganopolski, S. Murakami, B. Otto-Bliesner, and W. Peltier (2007), The modern and glacial overturning circulation in the Atlantic ocean in PMIP coupled model simulations, *Clim. Past*, *3*(1), 51–64.

Winton, M. (2000), A reformulated three-layer sea ice model, *J. Atmos. Oceanic Technol.*, *17*, 525–531.

Wunsch, C. (2005), Speculations on a schematic theory of the Younger Dryas, *J. Mar. Res.*, *63*(1), 315–333.

Yin, J., R. Stouffer, M. Spelman, and S. Griffies (2010), Evaluating the uncertainty induced by the virtual salt flux assumption in climate simulations and future projections, *J. Clim.*, *23*, 80–96.

I. Bethke, C. Li, and K. H. Nisancioglu, Bjerknes Centre for Climate Research, Allégaten 55, N-5007 Bergen, Norway. (ingo.bethke@uni.no)